ADVANCING EARTH AND SPACE SCIENCES

JGR Biogeosciences

RESEARCH ARTICLE
10.1029/2024JG008687

Spatial and Temporal Shifts in Dissolved Organic Matter Character Across a Burned Stream Network

K. A. Wampler[1,2], K. D. Bladon[1,3], A. N. Myers-Pigg[2,4], and J. A. Roebuck Jr.[2]

[1]Department of Forest Engineering, Resources, and Management, Oregon State University, Corvallis, OR, USA, [2]Marine and Coastal Research Laboratory, Pacific Northwest National Laboratory, Sequim, WA, USA, [3]Department of Forest Ecosystems and Society, Oregon State University, Corvallis, OR, USA, [4]Department of Environmental Sciences, University of Toledo, Toledo, OH, USA

Key Points:

- The relationship between dissolved organic matter composition and burn severity depended on weather, landscape, and hydrology
- Aromatics increased with burn severity during the wetting, drying, and dry seasons likely due to shifts in biotic and abiotic processes
- Protein-like compounds increased at severely burned sites during the wet season, likely due to shifts in above-ground organic matter

Supporting Information:

Supporting Information may be found in the online version of this article.

Correspondence to:

K. A. Wampler,
katie.wampler@oregonstate.edu

Citation:

Wampler, K. A., Bladon, K. D., Myers-Pigg, A. N., & Roebuck, J. A., Jr. (2025). Spatial and temporal shifts in dissolved organic matter character across a burned stream network. *Journal of Geophysical Research: Biogeosciences*, *130*, e2024JG008687. https://doi.org/10.1029/2024JG008687

Received 16 DEC 2024
Accepted 10 JUN 2025

Author Contributions:

Conceptualization: K. D. Bladon
Data curation: K. A. Wampler
Formal analysis: K. A. Wampler
Funding acquisition: K. D. Bladon, A. N. Myers-Pigg
Methodology: K. A. Wampler, K. D. Bladon, A. N. Myers-Pigg
Project administration: K. D. Bladon, A. N. Myers-Pigg
Resources: K. D. Bladon, A. N. Myers-Pigg
Supervision: K. D. Bladon, A. N. Myers-Pigg
Visualization: K. A. Wampler

Abstract Increasing wildfire activity can impact the global carbon cycle, aquatic ecosystem health, and drinking water treatment through alterations in aquatic dissolved organic matter (DOM) composition. However, uncertainty remains about the spatial and temporal variability in wildfire effects on DOM composition. We sought to improve understanding of how burn severity affects stream DOM and how weather, hydrology, and landscape factors contribute to variability in post-fire DOM responses across space and time. Following a large 2020 wildfire in Oregon, USA, we collected water samples to quantify dissolved organic carbon and DOM optical properties at 129 stream sites across the fire-affected stream network. Sampling was repeated across seasonal hydrologic conditions to capture variation in hydrologic pathways and organic matter sources. We developed a PARAFAC model using excitation-emission matrices (EEMs) and used spatial stream network (SSN) models to determine how DOM composition changed across the stream network with burn severity. The greatest shifts in DOM composition were observed during the dry and wetting seasons, with an increase in aromatic DOM at higher burn severities. In contrast, an increase in protein-like DOM was observed during the wet season at higher burn severities. Drainage area, 31-day and 1-day antecedent precipitation, and baseflow index impacted the relationship between DOM composition and burn severity, which could partially explain the variability in post-fire DOM responses. Our study contributes a mechanistic understanding of how wildfire impacts DOM sources and composition, which is critical to predicting wildfire effects on aquatic biogeochemical cycling and preserving ecosystem health and source water quality.

Plain Language Summary There has been increasing concern about how wildfires affect our aquatic ecosystems and drinking water treatment. In particular, there is concern about how the composition and transport of organics on the landscape post-fire impact stream organic matter. However, there is currently a lot of variability in the impacts that have been reported. We aimed to better understand this variability by collecting stream samples across a burned stream network to see how the organic matter was changing across the streams and how the burn severity of fire affected that. Overall, we found that the impact of burn severity on the types of organic molecules varied by seasonal wetness. We found an increase in the complex organic molecules during the dry and wetting up periods at the more severely burned streams. Conversely, in the wet season we found an increase in protein-like organic matter at the more severely burned streams. Additionally, we determined that landscape and weather characteristics can impact the relationship between burn severity and the types of organic matter in streams. Our work suggests that it is critical to control for landscape and weather characteristics when measuring organic matter post-fire.

1. Introduction

Streams play an important and active role in the global carbon cycle (Cole et al., 2007). It has been estimated that only ~20% of the carbon from the 5.1 Pg C yr^{-1} that streams, lakes, and wetlands receive from the terrestrial landscape reaches the ocean while the remainder is either stored in aquatic sediments or outgassed as CO_2 (Drake et al., 2018). A critical component of this carbon is dissolved organic carbon (DOC), which can make up the majority (~64%) of carbon inputs from the landscape to aquatic systems (Fahey et al., 2005). DOC also makes up a large proportion of the carbon processed in streams, with an estimated 27%–45% of DOC removed through in-stream processes (Mineau et al., 2016).

DOC represents the carbon component of dissolved organic matter (DOM), a complex mixture of organic compounds which vary in structure and environmental reactivity. Due to its diverse nature, shifts in DOM

Writing – original draft: K. A. Wampler
Writing – review & editing: K. A. Wampler, K. D. Bladon, A. N. Myers-Pigg, J. A. Roebuck Jr.

composition can have substantial impacts on the environment. Past work has shown that DOM quantity and composition can affect CO_2 emissions from streams (Bodmer et al., 2016), impact aquatic ecosystem health (Reitsema et al., 2018), and increase the challenges and costs of drinking water treatment (Yang et al., 2015). DOM quantity and composition have been found to shift in response to landscape disturbances such as extreme weather events (Majidzadeh et al., 2017), insect and pathogen outbreaks (Mikkelson et al., 2013), forest harvesting (Yamashita et al., 2011), and wildfires (Roebuck Jr. et al., 2022).

Wildfires are of increasing concern in the Western US. Substantial shifts in wildfire regimes have led to larger and more severe wildfires due to climate change and shifts in forest management (Marlon et al., 2012; Wasserman & Mueller, 2023). Wildfires can affect in-stream DOM in several ways. First, wildfires consume organic matter in the vegetation and on the soil surface. During a fire, a large proportion of organic matter is volatilized and lost to the atmosphere; however, between 1% and 28% of the organic matter may be retained on the landscape as pyrogenic organic matter (PyOM), a product of incomplete combustion with varying reactivity based on combustion temperature (Forbes et al., 2006; Preston & Schmidt, 2006; Santín et al., 2015; Wagner et al., 2018). Wildfire can also impact organic matter transport through shifts in hydrologic cycling, with vegetation loss leading to increased net precipitation (Williams et al., 2019) and decreased evapotranspiration (Kang et al., 2024), generally leading to more water moving through hillslopes (Hallema et al., 2017) while shifts in soil characteristics can impact water flow paths and flow timing (Ebel & Moody, 2017; Jung et al., 2009). It is generally thought that these impacts from wildfire result in increases in streamflow through surface runoff and shallow pathways; however, more recent research has shown that wildfire can also increase lateral flow and groundwater contributions to streams through overall increases in water availability and preferential flow paths (Atwood et al., 2023; Jung et al., 2009; Onda et al., 2008; Rey et al., 2023; Stoof et al., 2014). Since DOM is primarily mobilized during high flow events (Raymond & Saiers, 2010), water flowing through distinct flow paths could potentially mobilize different sources of DOM and alter the quantity and composition of DOM transported from burned hillslopes to streams.

However, there remains much uncertainty about how wildfires impact in-stream DOM composition (Tshering et al., 2023). A relatively quick and inexpensive approach to characterizing DOM is with the use of optical measurements, such as UV-VIS absorption and 3D excitation-emission fluorescence. The fluorescence index (FI) is a common metric typically associated with microbially derived and nitrogenous DOM (McKnight et al., 2001), and recent studies have observed increases in FI in burned streams indicating potential utility of optical analyses in identifying post fire impacts on stream DOM (Crandall et al., 2021; Fischer et al., 2023; Hickenbottom et al., 2023; Hohner et al., 2016; Uzun et al., 2020). However, interpretations around the linkages between DOM optical properties and fire activity are challenging in part due to the limited number of post-fire studies that have analyzed DOM composition in streams, particularly since the majority of studies are in arctic and semi-arid regions (Chow et al., 2019; Crandall et al., 2021; Fischer et al., 2023; Hickenbottom et al., 2023; Hohner et al., 2016; Larouche et al., 2015; Parham et al., 2013; Rodríguez-Cardona et al., 2020; Uzun et al., 2020). While there is a relatively large body of work investigating the DOM composition of ash and soil leachates (i.e., Cawley et al., 2018; Chen et al., 2020, 2023; Revchuk & Suffet, 2014), we know that DOM can be transformed while being transported through soils to streams through selective sorption (Kothawala et al., 2012), microbial degradation (Roth et al., 2019), and photodegradation (Egan et al., 2023). Such transformations could limit the comparability of laboratory-based leachate studies to stream and watershed observational studies post-fire.

Past work on both DOC concentrations and DOM composition has shown that the post-fire response can be highly variable and complex across both space and time (Tshering et al., 2023), highlighting the need for more work to explore the causes of this variability. A recent study investigating DOM composition across Canada reported no common effect of disturbance relative to the variability across different landscapes and climate, suggesting that disturbance effects may be more locally dependent (Orlova et al., 2024). Indeed, while fire characteristics are identified as the primary driver of the variability in responses (Raoelison et al., 2023), there is evidence that the variability in DOC concentrations can decrease across space and time as burn severity increases (Wampler et al., 2024c). This result suggests that there may be a more complex interaction between wildfire characteristics, landscape characteristics, hydrology, and climate that could influence the variability in post-fire DOM responses. Thus, it is critical to further explore how landscape and climate factors may interact with fire characteristics, such as burn severity, to modulate the post-fire response of DOM composition.

This work builds upon existing work in the same sub-basin (Wampler et al., 2024c), using DOC data collected at the same time as this study, which explored the impacts of burn severity on DOC concentrations across seasonal

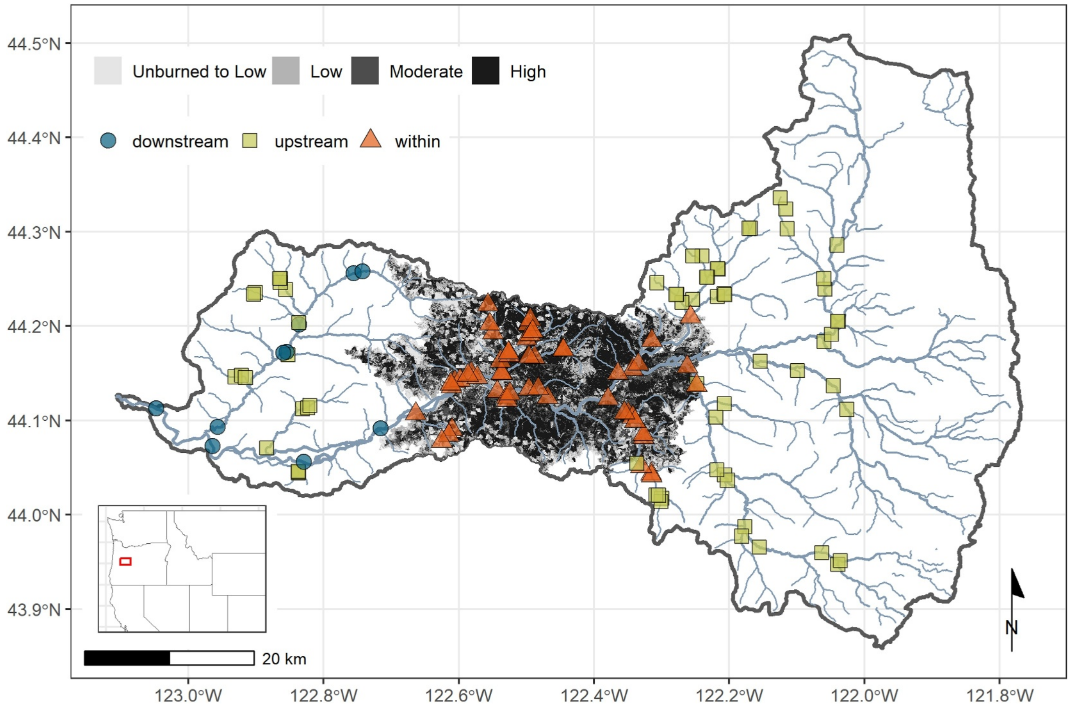

Figure 1. The McKenzie River sub-basin, Oregon USA (U.S. Geological Survey, 2020) with the burn severity map of the 2020 Holiday Farm wildfire (MTBS Project, 2021) and the stream sampling sites distributed across the stream network. The shapes indicate the location of each water sampling site relative to the Holiday Farm wildfire.

wetness conditions. Overall, in that work, DOC concentrations were determined to be more strongly related to baseflow index than burn severity, with strong seasonal variability in the impact of burn severity. Decreases in DOC concentration with burn severity were observed primarily during the wetting season.

In our study, we aimed to answer the following questions: (a) How does burn severity influence DOM composition in streams? (b) What landscape, hydrologic, climate, and wildfire variables best explain the variability in DOM composition across a burned stream network? (c) What landscape, hydrologic, and climate variables impact the relationship between burn severity and DOM composition?

2. Materials and Methods

2.1. Study Area

Our study occurred in the McKenzie River sub-basin (HUC 17090004), a 3,461 km^2 watershed on the Western slopes of the Cascade Mountains in Oregon, USA (Figure 1). The sub-basin ranges in elevation from 111 to 3,149 m with a median elevation of 954 m. The sub-basin has a mean slope of 16° with a maximum slope of 50°. It is located in a Mediterranean climate with cool wet winters and warm dry summers. Average annual precipitation across the basin ranges from 1,000 to 3,500 mm due to orographic effects, with an average precipitation of 2,200 mm (PRISM Climate Group, 2024). The 30-year (1991–2020) normal annual maximum temperatures across the basin ranged between 5.3 and 17.6°C while the 30-year normal annual minimum temperatures ranged between −5.0 and 5.8°C (PRISM Climate Group, 2024). The sub-basin is primarily forested, with ~80% of the area classified as forested, primarily with Douglas-fir (*Pseudotsuga menziesii*) and Western hemlock (*Tsuga heterophylla*) (Dewitz, 2021; Kagan et al., 2019). The upper two thirds of the sub-basin are mostly U.S. Forest Service land while the lower third of the basin is a combination of private residential land, commercial forestry, and agriculture. The geology of the sub-basin is primarily volcanic, with relatively young volcanics in the upper third of the basin, characterized by shallow slopes. The soils typically have extremely high infiltration capacity rates leading to deep subsurface flow paths and relatively large inputs of deep groundwater to streams. Comparatively, the lower two-thirds of the basin are comprised of older volcanics, which typically have steeper slopes with deeper organic soils and shallower flow paths where lateral flow paths dominate (Jefferson

Table 1
The Timing and Weather Conditions of Each Sampling Campaign

Season	Sampling date	Start time (PST)	End time (PST)	Storm precipitation depth (mm)	Average precipitation intensity (mm hr^{-1})	API 1 (mm)	API 7 (mm)	API 31 (mm)	Sites sampled
Wetting	1 Nov. 2022	5:30	17:15	7.6	0.6	14.0	45.7	123.7	126
Wet	13 March 2022	7:00	15:15	16.5	2.0	9.9	54.4	202.4	96
Drying	11 June 2023	6:30	17:30	0.0	0.0	0.0	0.5	17.5	117
Dry	11 Sept. 2023	6:45	17:15	0.0	0.0	0.0	0.0	18.0	78
Wetting	26 Sept. 2023	6:30	16:00	0.0	0.0	11.4	22.1	38.6	95
Wet	9 Dec. 2023	7:45	16:30	0.5	0.1	0.5	268.5	406.1	79
Drying	5 May 2024	6:30	15:30	11.9	1.3	21.6	108.7	231.9	94

et al., 2006; Tague & Grant, 2004). Since 1984, wildfires in the basin have been small and have generally occurred in the higher elevation headwater catchments. However, in fall 2020 the Holiday Farm Wildfire burned 18% of the sub-basin, with the wildfire located in the middle of the sub-basin, burning on both sides of the mainstem McKenzie River. This wildfire burned at relatively high severity with the burn classified as 9.2% unburned to low, 26.9% low, 29.4% moderate, and 33.3% high severity (MTBS Project, 2021).

2.2. Site Selection and Sample Collection

To investigate the impact of wildfire on dissolved organic matter (DOM) composition, we collected water samples from streams across the McKenzie River sub-basin starting in 2022, 2 years post-fire. Stream sampling sites were chosen to encompass the broad variability in climate, landscape, and wildfire characteristics across the basin. We selected sites that were near confluences to allow sampling upstream and downstream of tributaries and tried to select sites near roads for accessibility. We sampled 129 stream sites across the stream network with 65 sites upstream of the wildfire, 54 sites within the wildfire perimeter, and 10 sites downstream of the fire. However, because of accessibility issues, such as those due to high flows and/or wildfire restrictions from additional wildfires, the number of sites varied somewhat across sampling campaigns. We performed seven synoptic sampling campaigns between 2022 and 2024, where for each synoptic effort, we collected water samples from all the sites within a single day to enable us to capture a snapshot of DOM composition across the basin during that day. The sampling campaigns were spread across hydrologic wetness conditions or hydrologic seasons to capture the seasonal variability in DOC and DOM dynamics. Specifically, we collected samples once in the wetting, wet, drying, and dry seasons during the second to third-year post-fire and repeated this sampling once during the wetting, wet, and drying seasons in the third to fourth-year post-fire (Table 1).

Stream samples were collected from sections of the stream where water was highly mixed using extendable grab samplers. We collected ∼200 mL of water at each site. Samples were typically field filtered using a 0.2 μm PES syringe filter into triple rinsed acid washed HDPE bottles. However, for turbid samples, a larger sample volume was collected and stored in a cooler for transport to the laboratory where it was vacuum filtered using 0.2 μm PES disk filters within 24 hr of collection. In the lab, each sample was separated into separate bottles to enable quantification of optical properties and dissolved organic carbon (DOC) concentrations. Samples for DOC concentration were stored at 4°C until analysis, which generally occurred within 7 days of collection. However, when it was not possible to run DOC samples within a week of collection, samples were frozen at −15°C until they could be analyzed. Our samples generally had low DOC concentrations and, as such, freezing of samples would not be expected to significantly impact the DOC measurements (Fellman et al., 2008; Tupas et al., 1994). Water samples for optical measurements were stored at 4°C and samples were analyzed within 14 days of collection.

2.3. Water Quality Analysis

We measured DOC concentrations using a Shimadzu TOC-VCSH combustion analyzer, which measures non-purgeable organic carbon with an infrared detector. We also collected simultaneous absorbance and fluorescence optical measurements of each sample using a Horiba Aqualog equipped with an autosampler. Absorbance was collected from 240 to 800 nm at 3 nm intervals. Similarly, fluorescence in the form of excitation emission matrices (EEMs) was collected from excitation and emission wavelengths of 240–800 nm at 3 nm intervals. Optical data were processed using the *fewsdom* package in *R* (R Core Team, 2024; Wampler, 2023). Samples were blank corrected using a blank of MilliQ water, corrected for inner filter effects, and normalized to Raman units. The first and second order Rayleigh lines and first and second order Raman lines were removed from the spectra, the Raman lines were filled via interpolation. Lastly, the fluorescence intensity was normalized to 1 mg L^{-1} DOC using the measured DOC concentration for each sample to prevent fluorescence signal strength from affecting subsequent analyses (Murphy et al., 2013). Analysis of DOC results can be found in Wampler et al. (2024c).

2.4. Site Level Characteristics

To determine the site-level landscape, hydrologic, climate, and fire characteristics, we extracted polygons for the upstream contributing area for each site using StreamStats batch processing tool (U.S. Geological Survey, 2019). We then used zonal statistics with geospatial rasters describing our landscape, climate, and fire characteristics of interest to determine the average value across the watershed area upstream of each sampling site. Variables included annual precipitation, minimum and maximum temperature (PRISM Climate Group, 2024), burn severity (MTBS Project, 2021), percent forest (Dewitz, 2021), baseflow contact time and recharge depth (Schwarz et al., 2018), baseflow index (U.S. Geological Survey, 2003), aridity index (Trabucco & Zomer, 2019), elevation, slope, and topographic wetness index (U.S. Geological Survey, 2000), and available water capacity and soil clay (USDA NRCS, 2016). We also included some non-spatially explicit variables such as hydrologic season (i.e., wetting, wet, drying, dry) to broadly describe the hydrologic regime at the time of sampling. Similarly, we also included basin area (U.S. Geological Survey, 2019) and antecedent precipitation for the day samples were collected (i.e., API1, API7, API31). Antecedent precipitation was calculated using 15-min precipitation (rain and snow) records from the PRIMET precipitation station in the HJ Andrews Experimental Forest (Daly, 2024). We calculated API1 as the sum of precipitation in the 24 hr before the start of sampling, API7 as the sum of precipitation in the 7 days before the start of sampling, and API31 as the sum of precipitation in the 31 days before the start of sampling. See Table S1 in Supporting Information S1 for more details on these variables and data sets.

Burn severity was calculated using the Holiday Farm wildfire burn severity layer from Monitoring Trends in Burn Severity (MTBS Project, 2021). Similar to the other raster layers, we calculated the average difference in normalized burn ratio (dNBR) for the upstream area of each site where unburned areas were assigned a dNBR of 0. To facilitate additional comparisons across sites we also used the average dNBR to classify each site into a burn severity group (i.e., unburned, low, moderate, high). Classifications were determined using the burn severity thresholds determined by MTBS for the Holiday Farm wildfire, where dNBR values between 0 and 40 were classified as unburned, 41 and 320 were classified as low severity, 321 and 660 were classified as moderate severity, and values greater than 660 were classified as high severity.

To reduce multicollinearity in our potential explanatory variables, we calculated the Spearman correlations between variables. For variable pairs that were highly correlated ($\rho > 0.6$), we determined which variable was most highly correlated on average with our PARAFAC components. This variable was then used for the additional analysis, with the other correlated variable removed from further analysis (Figure S2 in Supporting Information S1). Final variables included for further analysis included basin area, 31-day antecedent precipitation, 1-day antecedent prediction, percent forest, contact time, baseflow index, topographic wetness index, available water capacity, aridity index, annual precipitation, and burn severity.

2.5. Statistical Analysis

We used our processed, DOC normalized EEMs to develop a parallel factor analysis (PARAFAC) model using the *staRdom* package in *R* (Pucher et al., 2019), which statistically separates individual fluorophores. PARAFAC models perform better and are more stable when there is more variability across samples to allow better separation of the fluorophores or PARAFAC components. To produce a better, more stable model, we included additional

EEMs measurements collected in the McKenzie River sub-basin between 2021 and 2022, which we collected before the spatial stream network study started (Wampler, Boise, et al., 2024; Wampler et al., 2024a). Additionally, to prevent erroneous peaks below the 1:1 excitation-emission line, which are not physically possible, we replaced all fluorescence values below the Raleigh scatter line with a value of zero (Thygesen et al., 2004). To fit our PARAFAC model we used non-negative constraints, 30 random starts, 10,000 maximum iterations, and a convergence tolerance of 10^{-8}. We tested models using between four to eight components. We chose the six-component model since it maximized the model fit without having significant drops in its ability to converge. Our final model explained 99.4% of the variation in our EEMs and our model was verified using split-half analysis (Wampler et al., 2024a, Figure S1 in Supporting Information S1). We used the open-source database OpenFluor (Murphy et al., 2014) to compare our PARAFAC components with similar components reported in the literature. The rest of our data analysis was performed using the relative proportion of each of the six PARAFAC components in each sample.

To examine the PARAFAC components in multivariate space, we performed a principal component analysis (PCA) on the six components using the "prcomp" function in *R* where all components were scaled to have a unit variance (R Core Team, 2024). The "envfit" function from the *vegan* package (Oksanen et al., 2024) was used to fit the site-level landscape, hydrologic, climate, and fire variables to the PCA ordination. To determine if there were differences in the burn severity groups in the multivariate space, we used a PERMANOVA based on Euclidean distances via the "adonis2" function in the *vegan* package (Oksanen et al., 2024). Sampling date was used for strata to account for the repeated sampling by constraining the shuffling of values between each sampling date. A pairwise post hoc test was performed using the "pairwiseadonis2" function in the *pairwiseAdonis* package (Arbizu, 2024). For all permutation-based tests we used 999 permutations.

2.5.1. Spatial Stream Network Models

To determine the relationship between burn severity and the PARAFAC components, we used spatial stream network (SSN) models (Ver Hoef et al., 2006; Ver Hoef & Peterson, 2010) to develop linear relationships between burn severity and each component while accounting for the spatial autocorrelation due to sites being connected on a stream network. SSN models are an extension of generalized linear regression models, which include additional random variables accounting for the spatial autocorrelation. Specifically, an SSN model can incorporate tail-up autocorrelation, which accounts for the distance between flow-connected sites, weighted by watershed area. It can also include tail-down autocorrelation, which consider the distance between all points on the network, using distances along the stream network. Additionally, the model can also incorporate Euclidean distances, which measure the straight-line (2D) distance between points, independent of the stream network. Each autocorrelation type can then be described using different mathematical models.

SSN models were built using the STARS toolbox in ArcMap (Peterson & Ver Hoef, 2014) and the *SSN2* package in *R* (Dumelle et al., 2024). Since our data were constrained between 0 and 1, we used the beta-family in the "ssn_glm" function to produce beta-family generalized linear models. To fit the SSN models, we first determined the best autocorrelation structure to use by examining the Torgegrams (Zimmerman & Ver Hoef, 2017) and then compared the Akaike information criterion (AIC) values across candidate models. Once the autocorrelation structure was determined, we selected the best model for each autocorrelation type by testing all possible combinations and selecting the combination that resulted in the lowest AIC value.

We built two SSN models for each PARAFAC component. One model included only burn severity group (unburned, low, moderate, and high) and the other model included burn severity group, season, and the interaction between the two. Both models used site as a random variable to account for the repeated samplings at each site. To determine if there was evidence that coefficients were not zero, we used the z-score and *p*-values from the Wald test in the summary output. These models were used to determine the average contribution of each component to total fluorescence for each burn severity group since they accounted for the repeated sampling and spatial autocorrelation in our data.

2.5.2. Interactions With Burn Severity

While it would have been ideal to make a single model including all the site characteristics, unfortunately, inclusion of multiple interaction effects in the models was challenging to interpret. Thus, we first determined the most important variables in explaining differences in our PARAFAC components and then individually tested

Table 2
Descriptions of the Six Components From Our PARAFAC Model

Component	Excitation maximum (nm)	Emission maximum (nm)	Coble peak[a]	Percent of F_{max} (%)[b]
C1	<248	460	A	12.4–31.2
C2	<248 (308)[c]	409	A + M	10.1–31.7
C3	362	456	C	4.3–16.0
C4	272 (413)[c]	502	D	2.3–13.3
C5	<248 (278)[c]	340	T	5.6–31.4
C6	272	304	B	2.8–49.0

[a]Coble 1996. [b]The range in the percentage of total fluorescence (F_{max}) for each component. [c]Secondary maxima shown in parentheses.

their interactions with burn severity. The most important variables were determined using a modified version geographical random forest models from the *spatialML* package in *R* (Kalogirou & Georganos, 2024), which uses spatially weighted random forest models. In each spatial random forest, a local model was created for each site using only the data nearby, with the distance specified by the user. The forests were then averaged. We modified the "grf" function in the package to use stream network distances instead of Euclidean distance, where the stream network distances were extracted from our SSN models. However, stream network distances only provide the distance between any two points along the stream network. Thus, to account for flow connectedness we included a variable indicating if the two sites were flow connected. The geographical random forest models provided the average variable importance across all models using the permutation method, which was then used to determine the most important variables in predicting each PARAFAC component.

For each variable found to be more important than burn severity, we created an SSN model incorporating that variable, burn severity (represented by average dNBR), and their interaction. As with the other SSN models, we used the z-scores and p-values from the Wald test to assess whether the interaction effect was significant. Due to the computational demands of examining interactions with burn severity, we focused on three of the six PARAFAC components—C1, C2, and C6—which represent different pools of DOM (Table 2) and were associated with differences in burn severity. To further investigate the interaction between burn severity and the selected variables, we generated interaction plots, exploring how concurrent changes in burn severity and the selected variables impacted the relative percentage of the PARAFAC component.

3. Results

3.1. PARAFAC Components

PARAFAC modeling produced a valid six component model, explaining 99.4% of the variability in our data (Figure 2). C1 represented between 12.4% and 39.2% of the total fluorescence and likely consisted of small molecular weight, photo resistant compounds due to fluorescing in the UVC region (Ishii & Boyer, 2012; Stedmon et al., 2003, Table 2). C2 has been previously associated with terrestrial DOM that has been microbially transformed, is relatively resistant to biodegradation, and represented between 10.0% and 31.7% of total fluorescence (Ishii & Boyer, 2012; Pucher et al., 2021; Queimaliños et al., 2019; Shutova et al., 2014). C3, which made up 4.3%–16.0% of total fluorescence, had few matches in openFluor but it was similar to fluorophores that were identified as terrestrial DOM that is aromatic and of high molecular weight (B. Chen et al., 2018; Kim et al., 2022; Panettieri et al., 2020; Yamashita et al., 2011).

C4 represented 2.3%–13.3% of total fluorescence and was identified as a ubiquitous aromatic component similar to high molecular weight, photolabile fluorophores (Ishii & Boyer, 2012; Wünsch et al., 2017; Y. Zhou et al., 2019). C5 made up between 5.6% and 31.4% of total fluorescence and resembled what is traditionally identified as a protein-like component tryptophan (Cawley et al., 2012; Retelletti Brogi et al., 2020; Stedmon & Markager, 2005a). While this component is often associated with high molecular weight compounds derived from primary productivity and microbial activity (Cawley et al., 2012; Derrien et al., 2020; Harjung et al., 2023; Retelletti Brogi et al., 2019), it has also been associated with small molecular weight, aromatic components likely from senescent plant materials and the breakdown of lignins (DeFrancesco & Guéguen, 2021; Hernes et al., 2009;

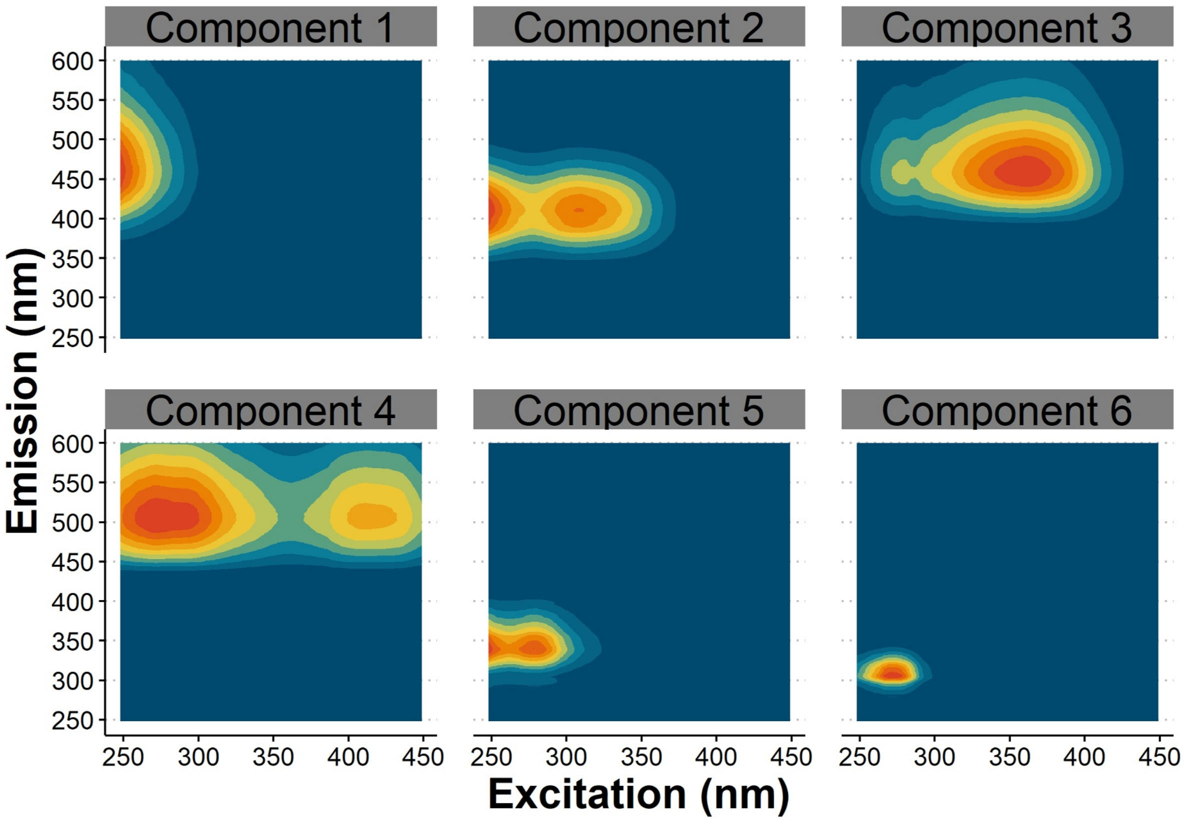

Figure 2. The components of our PARAFAC model based on EEMs collected from stream samples in the McKenzie sub-basin between 2021 and 2024. The intensity of the signal is represented by the colors from blue to red.

Lambert et al., 2017; Maie et al., 2007; Wheeler et al., 2017). C6 exhibited the largest variability, comprising 2.8%–49.0% of total fluorescence and resembled a protein-like component tyrosine (Graeber et al., 2012; Stedmon & Markager, 2005a; Yamashita et al., 2011). It is typically thought to be a more degraded protein-like component than C5 (D'Andrilli et al., 2019; Inamdar et al., 2011).

The variability across our six PARAFAC components was well described (89.0%) by the first two axes in our principal component analysis (PCA, Figure 3a). C1–C4 loaded positively on PC1 while C5 and C6 loaded negatively, suggesting that PC1 may reflect the degree to which the fluorescence was protein-like or aromatic. For PC2, C1, C2, and C5 loaded positively while C4 and C6 loaded negatively. While C2 loaded positively on PC1 and PC2, C6 loaded negatively on PC1 and PC2, suggesting these two components might be negatively correlated. A similar relationship was observed for C4 and C5.

Few environmental variables (Table S1 in Supporting Information S1) loaded strongly on PC1, with topographic wetness index (TWI) loading negatively and 31-day antecedent precipitation (API 31) loading positively (Figure 3b). Conversely, several environmental variables loaded strongly on PC2, with drainage area (DRNAREA), aridity (ARIDITY), dNBR (DNBR), subsurface residence time (CONTACT), 1-day antecedent precipitation (API1), and available water capacity (AWC) loading positively on PC2. Annual average precipitation (PRECIP), baseflow index (BFI), and percentage of basin that was forested (FOREST) all loaded negatively on PC2. Furthermore, some of the loadings of the environmental variables were quite similar to the loadings of the PARAFAC components. Specifically, topographic wetness index appeared negatively correlated with C1, drainage area appeared positively correlated with C5, and baseflow index appeared positively correlated with C6.

3.2. Shifts in DOM Composition With Burn Severity

We used spatial stream network models to determine how burn severity affected the relative percentage of each PARAFAC component. Using models with only burn severity as an explanatory variable, we determined that

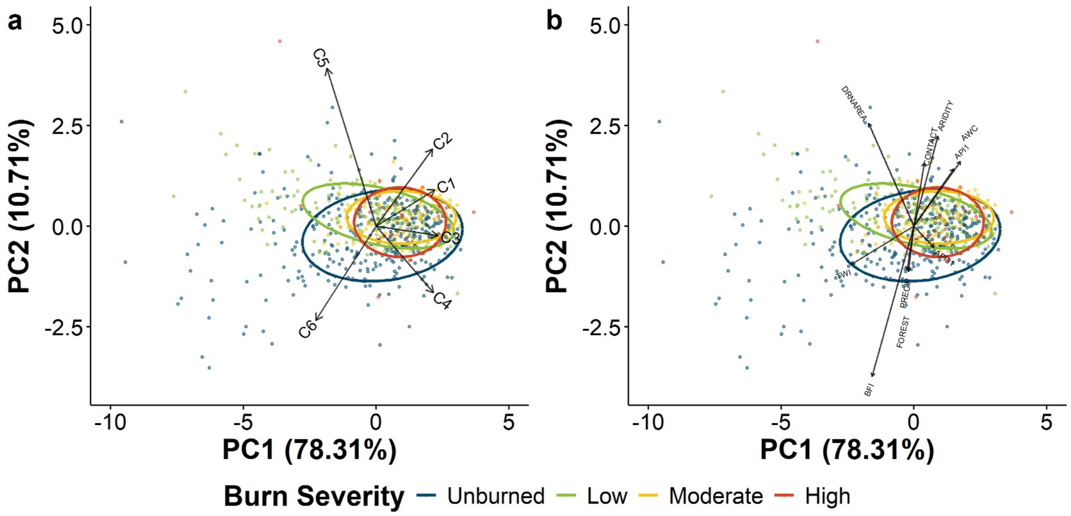

Figure 3. Biplots of a principal component analysis of the six components of our PARAFAC model where each point is a stream sample taken between 2023 and 2024 in the McKenzie River sub-basin, colored by burn severity group. The ellipses show the inner 75% of the data. The arrows show (a) the loadings for the six components and (b) the loadings of additional environmental factors.

burn severity alone was a very poor predictor of DOM composition, with pseudo R^2 values ranging from <0.001 to 0.003 (Table S2 in Supporting Information S1). Furthermore, the only burn severity group with evidence of being different from the unburned group was moderate severity, with a 1.4% increase in C1 ($p = 0.059$, z = 1.89) and 2.9% decrease in C6 ($p = 0.016$, z = −2.40) predicted.

PERMANOVA results indicated despite no distinctive visual separation between burn severity groups in our PCA (Figure 3) there was strong evidence that the groups were statistically different ($F_{3,681} = 16.391$, $p = 0.001$). Post-hoc pairwise testing provided further evidence ($p < 0.05$, Table S3 in Supporting Information S1) that the burn severity groups were all different except for the moderate and high severity groups ($F_{1,161} = 0.580$, $p = 0.364$). Specifically, the moderate and high burn severity groups were positivity shifted on the PC1 axis compared with the unburned and low severity groups (Figure 3), which suggested an increase in aromatic DOM. However, it should be noted that in unbalanced designs, when the larger group has greater variance, as in our study, PERMANOVA p-values can be deflated; thus, there is some uncertainty in the strength of statistical evidence that the groups are indeed different (Anderson & Walsh, 2013).

It appeared that shifts in DOM composition with burn severity were strongly seasonally dependent (Figure S3 in Supporting Information S1), though it should be noted that there was some overlap in the storm depth and antecedent precipitation across seasons (Table 1). Due to the seasonal dependence of DOM, we also determined the differences in the relative percentage of F_{max} for each component between burn severity groups for each season separately using SSN model with both burn severity and season (Table 3). Relative to the unburned group, the low severity group had less aromatic DOM (0.3%–1.7%) and more protein-like DOM (1.4%–2.6%) during the wetting season. In the wet season, the low severity sites were similar to the unburned, with minimal (≤0.4%) differences. During the drying and dry seasons, aromatic DOM was increased relative to the unburned group (drying: 0.4%–1.5%, dry: 0.0%–2.6%), with decreases in protein-like C6 (drying: 2.2%, dry: 4.6%).

The moderate severity group had the biggest differences from the unburned group. During the wetting, drying, and dry seasons there was more aromatic DOM, with increases in C1-C4 (−0.1%–5.3%) and decreases in C5 and C6 (0.0%–9.5%, Table 3). This trend was reversed in the wet season where C1-C3 were decreased somewhat (0.2%–0.6%) while C6 increased by 2.2%. Overall, the largest differences were observed for components C1 (5.3%) and C6 (−9.5%) during the dry season.

The high severity group was quite similar to the moderate severity group. Aromatic C1–C4 was increased (0.1%–3.9%) and protein-like C5 and C6 were decreased (0.7%–5.9%) during the wetting, drying, and dry seasons. During the wet season, aromatic C1–C4 were decreased (0.4%–1.8%) while protein-like C5 and C6 were

Table 3
Changes in PARAFAC Components Across Burn Severity and Season[a]

			Difference from unburned (%)			
Component	Pseudo R^2	Burn severity	Wetting	Wet	Drying	Dry
C1	0.152	Low	−1.7	0.2	1.5	2.6
		Moderate	2.0	−0.3	0.6	5.3
		High	0.6	−1.8	1.9	3.9
C2	0.163	Low	−0.3	0.0	0.7	0.6
		Moderate	1.2	−0.6	0.1	1.9
		High	1.0	−0.5	0.6	1.4
C3	0.231	Low	−0.9	0.1	0.8	0.4
		Moderate	0.8	−0.2	0.7	1.9
		High	0.3	−0.8	0.8	1.3
C4	0.134	Low	−0.7	0.1	0.4	0.0
		Moderate	0.5	0.0	−0.1	0.9
		High	0.7	−0.4	0.1	1.1
C5	0.090	Low	1.4	−0.4	−0.8	1.0
		Moderate	−0.3	0.0	−0.4	−0.5
		High	−0.7	2.0	−0.8	−1.5
C6	0.256	Low	2.6	0.2	−2.2	−4.6
		Moderate	−5.2	2.2	0.0	−9.5
		High	−3.5	1.7	−2.2	−5.9

[a]Table shows the changes in the average relative percentage of each PARAFAC component from the unburned group for low, moderate, and high burn severity determined by the seasonal spatial stream network models. See Table 2 for the range in relative percentage observed for each percentage.

increased (1.7%–2.0%). Just like the moderate severity group, the largest differences were observed for components C1 (3.9%) and C6 (−5.9%) during the dry season.

Based on these results, and to reduce complexity and computational resources, we chose to focus the rest of the analysis on C1, C2, and C6. These components likely represent different sources of DOM, had some of the strongest relationships with burn severity (Table 3), and had the largest differences across burn severity groups (Table 3).

3.3. Factors Controlling DOM Composition Across the Stream Network

For C1, C2, and C6, we created geographically weighted random forest models using the 11 climate, hydrologic, landscape, and wildfire variables selected from our down selection procedure (Figure S2 in Supporting Information S1), in addition to season and flow connectedness, as explanatory variables. Variable importance results from our geographically weighted random forest models showed that 31- and 1-day precipitation, baseflow index, aridity index, and basin area were consistently some of the most important variables in each model. However, the relative importance of these variables were unique for each component (Figure 4). C1 appeared to be driven by a combination of climate, hydrologic, and landscape variables. The 31-day antecedent precipitation, baseflow index, and basin area were all roughly of equal importance to C1. C2 appeared to be highly driven by wetness changes with 31- and 1-day antecedent precipitation and season as the most important variables. Conversely, C6 seemed to be strongly driven by baseflow index. Notably, burn severity ranked roughly in the middle of the variable importance across all three components.

For each component, we tested the interaction between burn severity (as average dNBR) and all variables that ranked as more important than burn severity using spatial stream network models. There was strong evidence ($p < 0.01$) of an interaction between 1-day antecedent precipitation and burn severity for C2 and C6 (Figures 5a and 5b). Despite this, the predicted change in the relative percentage of each component was not very large compared with the variability we observed across sites (Table 2), with C2 ranging from 17% to 20% and C6 ranging from 6% to 16%. Interaction models predicted increased C2 and decreased C6 as 1-day precipitation and burn severity increased, with the highest concentrations for C2 and lowest concentration for C6 predicted when 1-day precipitation was greater than 20 mm and average dNBR was above 600 (high severity). Additionally, the

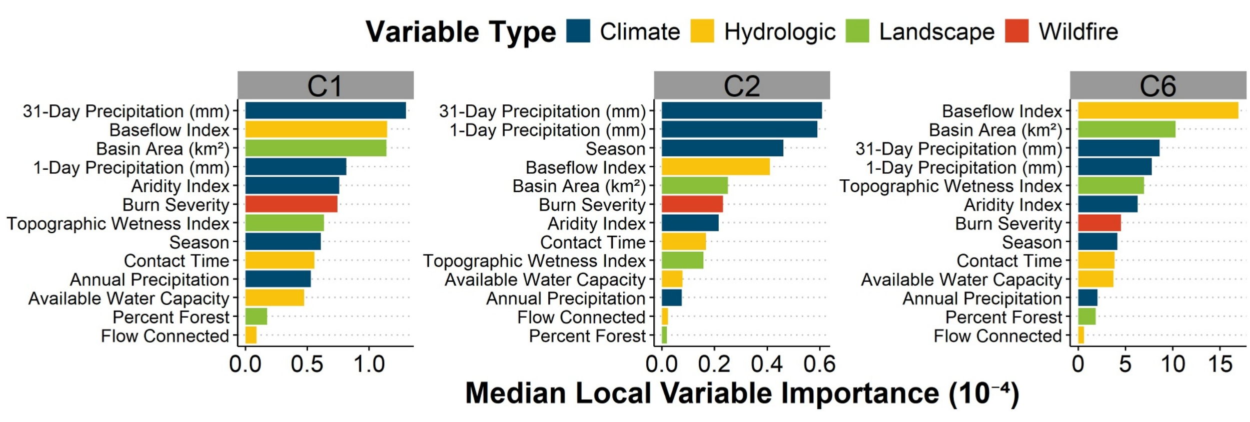

Figure 4. Importance of climate, hydrologic, landscape, and wildfire variables in describing the relative percentages of C1, C2, and C6 determined using the median of the local variable importance from geographically weighted random forest models.

Journal of Geophysical Research: Biogeosciences 10.1029/2024JG008687

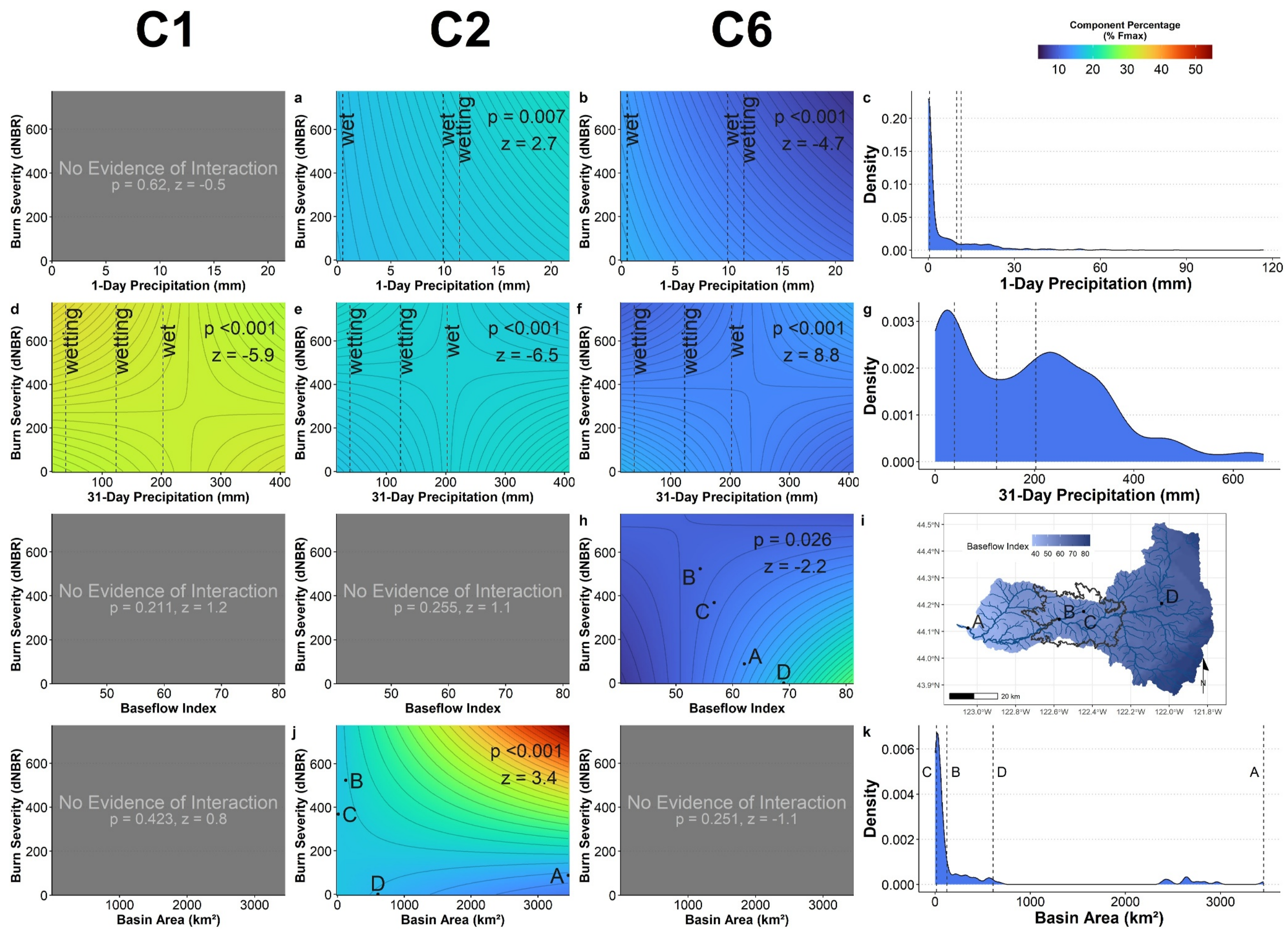

Figure 5. Interaction plots showing how concurrent changes in burn severity (on the *y*-axis) and landscape, hydrologic, and climate variables (on the *x*-axis) are predicted to influence the relative percentage of individual PARAFAC components (indicated by the color scale and contours). We tested all interactions between burn severity and 1-day and 31-day precipitation, baseflow index, and basin area, for components C1 (d), C2 (a, e, j), and C6 (b, f, h). Only significant interactions ($p < 0.1$) are plotted. Patterns that change across both the *x*- and *y*-axes suggest that the impact of burn severity is not constant, varying with the value of the landscape factor on the *x*-axis. To aid in interpretation, example sites are indicated with letters a–d for baseflow index (h) and basin area (j) which correspond to the example sites shown in (i, k). The dashed lines indicate example precipitation depths that occurred during sampling campaigns for 1-day and 31-day precipitation. The distribution of the variable over the basin (baseflow index and drainage area) or over time (31- and 1-day precipitation) is shown in (c, g, i, and k).

model predicted that C2 and C6 were more sensitive to changes in burn severity when 1-day precipitation was higher.

There was also strong evidence ($p < 0.001$) of an interaction between 31-day antecedent precipitation and burn severity for all three components (Figures 5d–5f). However, similar to 1-day precipitation, the range of predicted change in relative component percentage was not large compared to the observed variability across sites. Interaction models predicted changes between 30% and 35% for C1, 17% and 20% for C2, and 10% and 16% for C6. Interaction plots showed a complex relationship between 31-day antecedent precipitation and burn severity. When 31-day precipitation was below ∼250 mm, C1 and C2 increased and C6 decreased with increasing burn severity. Conversely, when 31-day precipitation was above ∼250 mm, the reverse was predicted, with C1 and C2 decreasing and C6 increasing with increasing burn severity.

While baseflow index was more important than burn severity for all three components, there was only evidence of an interaction effect for C6 ($p = 0.026$). Despite having weaker evidence of an interaction than 1- and 31-day precipitation, the range of predicted changes in C6 was larger, with a range of 7%–25%. Changes in C6 were relatively insensitive to changes in burn severity for baseflow indices below 50, and the effect of baseflow index was minimal for average dNBR values above 600 (high severity), with both predicting low percentages of C6

(Figure 5h). Conversely, at high baseflow indices, the model predicted larger changes in C6 for changes in burn severity, with less C6 at higher burn severities.

Lastly, there was evidence of an interaction effect between burn severity and basin area for C2 ($p < 0.001$, Figure 5j). The predicted changes in the relative percentage of C2 were the largest across all the interaction effects, ranging from 12% to 55%. C2 did not vary much across the burn severity gradient when basin area was less than ~500 km^2. As basin area increased, the importance of burn severity also increased. At large basin areas, the model predicted increased C2 with increasing burn severity.

4. Discussion

4.1. Shifts in DOM Composition With Burn Severity

In our study of the McKenzie River sub-basin in the Western Cascades of Oregon, USA, we observed a greater proportion of C1, small molecular weight, photo-resistant compounds, in stream water samples from moderate and high burn severity sites compared with unburned sites during the wetting, drying, and dry seasons (Table 3). During these seasons, it is likely that photo-production played a role in influencing C1 production (Stedmon et al., 2007; Y. Zhou et al., 2019), which is consistent with multiple studies, including ours, that have noted increases in C1-like molecules during the warmer months with longer day lengths (Ishii & Boyer, 2012; Kothawala et al., 2014). In our study, we expected greater photo-production in areas burned at higher severity due to the loss of forest canopy, which enabled increased solar insolation (Lentile et al., 2007, Table 3). Additionally, the increase in C1 at the sites burned at higher severity could be due to photo-degradation of pyrogenic organic matter (PyOM), which can result in smaller molecular weight, less aromatic molecules, including C1 (Ishii & Boyer, 2012; Wagner & Jaffé, 2015). Similar to our results, past work on soil leachates collected between 3 and 36 months following a wildfire in China also linked C1 to PyOM, with a similar increase in C1-like fluorophores (Yin et al., 2024). The link between C1 and photo production is also supported by the minimal shifts in C1 we observed at low and moderate severity during the wet season, where we would expect less photo-activity due to shorter day lengths and cloudy weather (Table 3).

However, it is likely that photo-degradation was not the only process affecting C1 across the stream network, as we observed a decrease in C1 in water from the high burn severity sites during the wet season (Table 3). This decrease could be due to decreased sources of organic matter at the high severity burn sites, as the primary source of C1 during the wet season was likely from soil organic matter (Ishii & Boyer, 2012; Stedmon & Markager, 2005a). Past work has observed decreased soil organic matter in the O horizon following moderate and high severity burns (Certini et al., 2011; Hatten & Zabowski, 2010). This is also consistent with results of our PCA which illustrated that C1 was negatively related to topographic wetness index, suggesting that C1 may be greater in areas with steeper slopes, likely due to shallower flow paths through more organic layers (Tetzlaff et al., 2009, Figure 3). Lastly, while not well supported by our data, the increase in C1 could be due to untransformed PyOM, as C1-like components have been observed to increase at moderate burn temperatures (175–450°C) in laboratory burning experiments of soil and litter, which were not subjected to photodegradation (Q. Zhang et al., 2023).

We also observed increased proportions of C2—representative of potentially microbially transformed, aromatic compounds—in water samples from moderate and high burn severity sites relative to unburned sites during the wetting, drying, and dry seasons (Table 3). This is consistent with laboratory experiments of wildfire-burned soil leachates and experimentally burned vegetation, where C2-like fluorophores were increased in burned leachates compared with unburned (Bravo-Escobar et al., 2024; Cao et al., 2024; Roebuck Jr. et al., 2024; Yin et al., 2024). Increases in C2 in our water samples were likely due to increased C2 in post-fire soils and litter, which was transported from burned hillslopes to the streams. This theory is consistent with the interaction we observed between burn severity and 1-day antecedent precipitation (Figure 5), where the highest C2 was predicted in severely burned areas with high 1-day precipitation. Such conditions would be conducive to elevated hillslope runoff through soils that would likely have elevated C2-like fluorophores.

We also hypothesize that increases in C2—potentially microbially transformed, aromatic compounds—were related to decreases in C6—tyrosine or protein-like components—based on results from our PCA, which showed a nearly inverse relationship between the two components (Figure 3). Indeed, C6 was lower in water samples from moderate and high burn severity sites during the wetting, drying, and dry seasons, which was the reverse of C2 (Table 3). Research from eucalypt forests and pine plantations in southwest Australia also illustrated

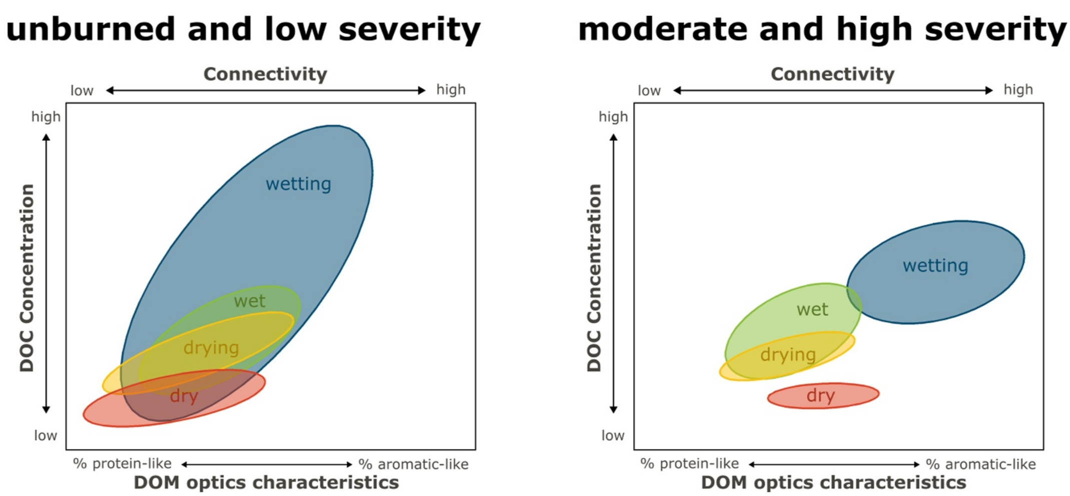

Figure 6. Conceptual model of seasonal shifts in DOC concentrations and DOM compositions at unburned and low severity and moderate and high severity. The conceptual model was based on our data, where the ellipses are based on the inner 50% of each group. The numeric axes were removed and replaced with descriptive axes. Figure was based on a figure by S. Singh et al. (2014) and DOC data from Wampler et al., 2024c.

a similar inverse relationship between protein-like fluorophores and C2-like components in post-fire soil leachates 4 months after wildfire (Bravo-Escobar et al., 2024). This increase in C2 and decrease in C6 could be related to transformations in soil organic matter composition due to the heat of the wildfire. In experimental open-air burns, Douglas-fir leachates exhibited a shift from C6-like DOM toward C2-like DOM with increasing burn severity (Roebuck Jr. et al., 2024). However, it is also possible that shifts in the DOM composition could have been influenced by microbial activity. The observed shifts in DOM composition may have occurred if microbes were preferentially using C6, which is biologically labile (D'Andrilli et al., 2019), while also producing C2, which is often linked to microbially transformed terrestrial organic matter (Ishii & Boyer, 2012; Lambert et al., 2016; Pucher et al., 2021). While production of C2-like components can be derived from degradation of other aromatic DOM components (Andrew et al., 2013), there is also evidence the C2 can be produced autochthonously from microbes (Fox et al., 2019; Stedmon & Markager, 2005b). Furthermore, while research has been limited, there is evidence that wildfires can have immediate and long-lasting influences on microbial communities, microbial activity, and microbial biomass by both direct and indirect shifts in the soil environment (Rodríguez et al., 2017; A. K. Singh et al., 2017).

4.2. Impacts of Burn Severity Vary Seasonally

4.2.1. Seasonality in Unburned Systems

At our unburned and low severity sites, we observed the most aromatic-like DOM (C1-C4) during the wetting season (Figure 6), which is consistent with previous work from the region (Hood et al., 2006). This is likely due to the build up of terrestrial organic matter on the landscape, which is then available for transport to streams as the basin rewets (Raymond & Saiers, 2010). As sources of DOM were reduced and the basin dried out, the DOM composition shifted toward more protein-like DOM (C5-C6, Figure 6), likely due to increased groundwater inputs, which tend to have a more protein-like composition due to selective sorption of more aromatic molecules (Shen et al., 2015).

4.2.2. The Wetting Season

The largest shifts in DOM composition across burn severity groups occurred during the dry and wetting seasons, with an increase in aromatic C1-C4 and decrease in protein-like C5 and C6 at moderate and high burn severities (Table 3). It was not surprising that the wetting season experienced larger shifts. Previous work in the basin found the largest decreases in DOC concentration during the wetting season post-fire, possibly due to loss of organic matter on the landscape or increased groundwater inputs (Wampler et al., 2024c). The wetting season has also been identified as a critical period of flushing following long dry periods where large pools of "potential" DOM that have built up on the landscape are transported to streams similar to the freshet period in the arctic (Mann et al., 2012; Raymond et al., 2007; Raymond & Saiers, 2010). Thus, small daily differences in DOM processing and accumulation on the landscape, when integrated over the entire dry period, likely result in the larger differences we observed in the wetting season.

4.2.3. The Dry Season

It was surprising that the dry season exhibited the largest differences in DOM composition across burn severity groups with an increase in aromatic C1-C4 and decrease in protein-like C5 and C6 at moderate and high burn severities (Table 3). Flows during the dry period tend to have a high proportion of groundwater and deep lateral subsurface flow (Smakhtin, 2001), which takes long flow paths through deeper soils, that are likely minimally affected by heat of the wildfire, so we would expect shifts in DOM composition to be minimal (Chicco et al., 2023; Knicker, 2007). However, that was not what we observed. Substantial differences in PyOM between burned and unburned sites was also observed during baseflows following a wildfire in Colorado, USA (Wagner et al., 2015). While they attributed this increase to inputs of soluble PyOM in surface soils, we would not expect surface soils to substantially impact the DOM composition of baseflows without alterations in soil processing or flow paths.

Thus the increase in aromatic-like DOM could be due to alterations in flow paths post-fire. Past work has found that wildfire can increase baseflows (Kinoshita & Hogue, 2015; Mahat et al., 2016) likely due to decreased ET post-fire (Kang et al., 2024). This increase in dry season water availability could lead to more shallow groundwater flow paths (Blount et al., 2020; Cardenas & Kanarek, 2014; Giambastiani et al., 2018), with the potential to shift the composition of the DOM that is transported toward more aromatic and less protein-like DOM (Lee & Lajtha, 2016). Similarly, the changes in DOM composition during the dry season could be due to post-fire alterations to the soil layers, reducing adsorption and processing of infiltrating DOM, allowing more aromatic DOM to reach the deeper soil layers and altering the composition of the groundwater. This is supported by our interaction plots (Figure 5), which suggest that we see the largest decreases in protein-like DOM at higher burn severities in areas with more groundwater inputs. An increase in C2 in groundwater sources is also consistent with the interaction between burn severity and drainage area (Figure 5), as the influence of groundwater often increases with basin area (Burgers et al., 2014; Creed et al., 2015; McGuire et al., 2014). Past work has noted increased preferential flow paths in burned soils (Atwood et al., 2023; Kopp et al., 2017; Stoof et al., 2014) which would decrease the interaction time between DOM and soils, potentially allowing more aromatic material to infiltrate to deeper layers. It has been hypothesized that shorter flow paths and shorter contact times are related to higher aromatic DOM and higher DOC concentration in groundwater (Inamdar et al., 2011; van Verseveld et al., 2008). Additionally, increased aromatics in deeper soil layers could be due to altered soil properties decreasing sorption of aromatics. Wildfire can cause an increase in soil pH due to ash inputs (Certini, 2005), and there is some evidence that aromatic materials are more soluble at higher pH's (Hrelja et al., 2022; Kalbitz et al., 2000).

Conversely, the shifts in DOM composition we observed during the dry season could be due to shifts in in-stream processing post-fire. Burned streams can have higher in-stream productivity due to increased nutrients, greater light availability, and warmer stream temperatures (Betts & Jones, 2009; Rhea et al., 2021; Robinson et al., 2005; Tuckett & Koetsier, 2016). While we would expect this to increase autochthonous sources of DOM, including C2, C5, and C6, we only observed an increase in potentially microbially derived C2 (Table 3). It is also possible that increased erosion during wetter periods could lead to storage of particulate PyOM in the stream channel which can then be weathered during the dry period, increasing solubility and increasing the proportion of aromatic DOM. Several studies have noted stores of eroded particulate PyOM stored in stream corridors (Bodí et al., 2014; Cotrufo et al., 2016; Moody & Martin, 2001), which could provide a continuous source of PyOM during the dry period, particularly C1 and C2 if they are products of photo and microbially degraded PyOM. This is consistent with the interaction between burn severity and drainage area (Figure 5), as we would expect more in-stream processing at larger basin scales (Creed et al., 2015). Additionally, past work has suggested that more deposition of PyOM material occurs at larger basin scales (Condon, 2013; Cotrufo et al., 2016), suggesting that perhaps larger streams have larger pools of PyOM to degrade.

4.2.4. The Wet Season

The wet season tended to exhibit the opposite trend from the other seasons, with increases in protein-like C5 and C6 and decreases in aromatic C1-C4 at moderate and high severities (Table 3). This seemed to be related to long-term antecedent conditions since we saw a similar shift in DOM composition across the 31-day precipitation interactions (Figure 5). An increase in protein-like DOM and decrease in aromatic DOM was observed in the initial flushes following wildfire in California, but it was not observed in subsequent flushes (Uzun et al., 2020). This increase was thought to be due to partial combustion products or post-fire microbial activity (Revchuk & Suffet, 2014; Uzun et al., 2020). Typically the wet season experiences an increase in aromatic DOM due to more shallow flow paths through organic layers and throughfall (Inamdar et al., 2011), so this decrease in aromatics at the higher burn severities could be reflective of decreased organic layers or loss of vegetation in the higher severity landscapes (Certini et al., 2011; Hatten & Zabowski, 2010; Miesel et al., 2015). Indeed, characterization of post-fire soils and litter layers noted an increased proportion of protein-like DOM in burned soils (Miesel et al., 2015). Additionally, the higher protein-like DOM could be due to more protein-like throughfall from early seral species in the recovering landscapes as past work has identified throughfall as an important source of storm streamflow (Inamdar & Mitchell, 2006). Furthermore, snowbrush litter (*Ceanothus velutinus*), a common early seral species post-fire in the Western Cascades (Brown et al., 2013), has been found to be enriched in soluble proteins and polyphenols (Uselman et al., 2012).

4.3. Potential Implications of DOM Composition Shifts

While the majority of shifts in DOM composition we observed across burn severity groups were relatively small (<5%, Table 3), the relative changes in PARAFAC components observed could still have environmental significance. For example, DOM composition has been previously linked to bioavailability, where a 1% increase in protein-like DOM resulted in a ∼1% increase in bioavailable DOM (Hosen et al., 2014). In forested streams in Europe, for a 1% increase in high molecular weight, aromatic organic matter was related to a ∼300 ppm increase in the partial pressure of carbon dioxide in streams, roughly a 10% increase (Bodmer et al., 2016). Water management can also be impacted; work in Australian water treatment plants determined that an increase of 1 in the ratio of aromatic DOM to protein-like DOM increased DOC removal by ∼20% (Shutova et al., 2014).

Overall, past work has found that DOM composition can exert strong controls on a wide range of ecosystem functions. For instance, the increase in complex, aromatic DOM we observed at higher burn severities (Table 3), has been related to increases in ecosystem respiration (Fuß et al., 2017), both increases and decreases in heavy metal complexation (Huang et al., 2022; Mueller et al., 2012; F. Zhang et al., 2021), shifts in bacterial abundance and diversity (Thuile Bistarelli et al., 2021; L. Zhou et al., 2021), and the formation of carbon disinfection byproducts (i.e., HAA and THM) during drinking water treatment (Fernández-Pascual et al., 2023).

We observed small, but still potentially impactful shifts in DOM composition between 2 and 4 years following wildfire. While much work on DOM composition has taken place in the first 2 years following wildfire (Crandall et al., 2021; Fischer et al., 2023; Hickenbottom et al., 2023; Hohner et al., 2016; Uzun et al., 2020), our work suggests that impacts of wildfire on DOM composition can be more long lasting. This is consistent with a growing body of research that has observed that wildfire can lead to long-term impacts on DOM (Chow et al., 2019; Rodríguez-Cardona et al., 2020; Santos et al., 2019). However, continued work is needed to more fully quantify the long-term recovery trajectories of DOM.

5. Conclusions

Using stream water samples collected at a high spatial resolution across a burned stream network we determined that DOM composition changed with increasing burn severity, with increases in aromatic DOM occurring during the wetting, drying, and dry seasons while increases in protein-like DOM occurred during the wet seasons (Figure 6). We also used spatial stream network models to explore how climate, hydrology, and landscape factors interact with burn severity to influence the DOM composition. Overall, we found that antecedent precipitation, baseflow index, and drainage area all modulated the relationship between DOM composition and burn severity, suggesting these are important variables to consider in designing future post-fire studies. While we cannot be certain of the mechanisms behind the shifts in DOM composition we observed, this work lays out several hypotheses of post-fire shifts in stream DOM, which could be further explored and validated in future work. Overall, while uncertainty remains about the implications of post-fire shifts in DOM composition, past studies suggest that even relatively minor shifts in DOM composition post-fire, as we observed, can still have substantial impacts on carbon cycling, aquatic ecosystem health, and source water quality that can create challenges for downstream drinking water treatment.

Data Availability Statement

The data and code that support the findings of this study are openly available at Scholars Archive at Oregon State University (Wampler et al., 2024a, https://ir.library.oregonstate.edu/concern/datasets/mc87q034m, https://doi.org/10.7267/mc87q034m; Wampler et al., 2024b).

Acknowledgments

We would like to thank all of the people who helped collect this data: Kelly Andrus, Alessandra Bertucci, Gillian Campbell, Brenna Cody, Ryan Cole, Weylin Crouch, Alex Foote, Bradley Gerdes, Indy Gerhardt, Jansen Ivie, Hyunwoo Kang, Katherine McCool, Spencer McMaster, Lorrayne Miralha, Humyra Murshed, Josiah Nelson, Emily Nussdorfer, Sam Ogle, Cedric Pimont, Will Potter, and Dave Roon—your help was invaluable. We would also like to thank Dustin Gannon for his help with the statistics in this paper. Funding to support this research was provided by the US Forest Service (agreement numbers 22-JV-11261952-071 and 23-JV-11261954-057) and the US Department of Energy (DOE), Office of Science, Biological and Environmental Research, Environmental System Science (ESS) program as part of the River Corridors Science Focus Area (54737) at the Pacific Northwest National Laboratory (PNNL). PNNL is operated for the DOE by Battelle Memorial Institute under contract DE-AC05-76RL01830.

References

Anderson, M. J., & Walsh, D. C. I. (2013). PERMANOVA, ANOSIM, and the Mantel test in the face of heterogeneous dispersions: What null hypothesis are you testing? *Ecological Monographs*, *83*(4), 557–574. https://doi.org/10.1890/12-2010.1

Andrew, A. A., Del Vecchio, R., Subramaniam, A., & Blough, N. V. (2013). Chromophoric Dissolved Organic Matter (CDOM) in the equatorial Atlantic Ocean: Optical properties and their relation to CDOM structure and source. *Marine Chemistry*, *148*, 33–43. https://doi.org/10.1016/j.marchem.2012.11.001

Arbizu, P. M. (2024). Pairwise Adonis: Pairwise multilevel comparison using Adonis. R. Retrieved from https://github.com/pmartinezarbizu/pairwiseAdonis

Atwood, A., Hille, M., Clark, M. K., Rengers, F., Ntarlagiannis, D., Townsend, K., & West, A. J. (2023). Importance of subsurface water for hydrological response during storms in a post-wildfire bedrock landscape. *Nature Communications*, *14*(1), 3814. https://doi.org/10.1038/s41467-023-39095-z

Betts, E. F., & Jones, J. B. (2009). Impact of wildfire on stream nutrient chemistry and ecosystem metabolism in boreal forest catchments of Interior Alaska. *Arctic Antarctic and Alpine Research*, *41*(4), 407–417. https://doi.org/10.1657/1938-4246-41.4.407

Blount, K., Ruybal, C. J., Franz, K. J., & Hogue, T. S. (2020). Increased water yield and altered water partitioning follow wildfire in a forested catchment in the Western United States. *Ecohydrology*, *13*(1), e2170. https://doi.org/10.1002/eco.2170

Bodí, M. B., Martin, D. A., Balfour, V. N., Santín, C., Doerr, S. H., Pereira, P., et al. (2014). Wildland fire ash: Production, composition and eco-hydro-geomorphic effects. *Earth-Science Reviews*, *130*, 103–127. https://doi.org/10.1016/j.earscirev.2013.12.007

Bodmer, P., Heinz, M., Pusch, M., Singer, G., & Premke, K. (2016). Carbon dynamics and their link to dissolved organic matter quality across contrasting stream ecosystems. *Science of the Total Environment*, *553*, 574–586. https://doi.org/10.1016/j.scitotenv.2016.02.095

Bravo-Escobar, A. V., O'Donnell, A. J., Middleton, J. A., & Grierson, P. F. (2024). Differences in Dissolved Organic Matter (DOM) composition of soils from native eucalypt forests and exotic pine plantations impacted by wildfire in Southwest Australia. *Geoderma Regional*, *37*, e00793. https://doi.org/10.1016/j.geodrs.2024.e00793

Brown, M. J., Kertis, J., & Huff, M. H. (2013). *Natural tree regeneration and coarse woody debris dynamics after a forest fire in the Western Cascade Range. Res. Pap.* U.S. Department of Agriculture, Forest Service, Pacific Northwest Research Station. https://doi.org/10.2737/PNW-RP-592

Burgers, H. E., Schipper, A. M., & Jan Hendriks, A. (2014). Size relationships of water discharge in rivers: Scaling of discharge with catchment area, main-stem length and precipitation. *Hydrological Processes*, *28*(23), 5769–5775. https://doi.org/10.1002/hyp.10087

Cao, X., Li, S.-A., Huang, H., & Ma, H. (2024). Wildfire impacts on molecular changes of dissolved organic matter during its passage through soil. *Environmental Science & Technology*, *58*(26), 11436–11446. https://doi.org/10.1021/acs.est.3c11056

Cardenas, M. B., & Kanarek, M. R. (2014). Soil moisture variation and dynamics across a wildfire burn boundary in a loblolly pine (*Pinus taeda*) forest. *Journal of Hydrology*, *519*, 490–502. https://doi.org/10.1016/j.jhydrol.2014.07.016

Cawley, K. M., Butler, K. D., Aiken, G. R., Larsen, L. G., Huntington, T. G., & McKnight, D. M. (2012). Identifying fluorescent pulp mill effluent in the Gulf of Maine and its watershed. *Marine Pollution Bulletin*, *64*(8), 1678–1687. https://doi.org/10.1016/j.marpolbul.2012.05.040

Cawley, K. M., Hohner, A. K., McKee, G. A., Borch, T., Omur-Ozbek, P., Oropeza, J., & Rosario-Ortiz, F. L. (2018). Characterization and spatial distribution of particulate and soluble carbon and nitrogen from wildfire-impacted sediments. *Journal of Soils and Sediments*, *18*(4), 1314–1326. https://doi.org/10.1007/s11368-016-1604-1

Certini, G. (2005). Effects of fire on properties of forest soils: A review. *Oecologia*, *143*(1), 1–10. https://doi.org/10.1007/s00442-004-1788-8

Certini, G., Nocentini, C., Knicker, H., Arfaioli, P., & Rumpel, C. (2011). Wildfire effects on soil organic matter quantity and quality in two fire-prone Mediterranean pine forests. *Geoderma*, *167–168*, 148–155. https://doi.org/10.1016/j.geoderma.2011.09.005

Chen, B., Huang, W., Ma, S., Feng, M., Liu, C., Gu, X., & Chen, K. (2018). Characterization of chromophoric dissolved organic matter in the littoral zones of Eutrophic lakes Taihu and Hongze during the Algal Bloom season. *Water*, *10*(7), 861. https://doi.org/10.3390/w10070861

Chen, H., Uzun, H., Chow, A. T., & Karanfil, T. (2020). Low water treatability efficiency of wildfire-induced dissolved organic matter and disinfection by-product precursors. *Water Research*, *184*, 116111. https://doi.org/10.1016/j.watres.2020.116111

Chen, H., Uzun, H., Tolić, N., Chu, R., Karanfil, T., & Chow, A. T. (2023). Molecular transformation of dissolved organic matter during the processes of wildfire, Alum coagulation, and disinfection using ESI(−) and ESI(+) FT-ICR MS. *ACS ES&T Water*, *3*(8), 2571–2580. https://doi.org/10.1021/acsestwater.3c00135

Chicco, J. M., Mandrone, G., & Vacha, D. (2023). Effects of wildfire on soils: Field studies and modelling on induced underground temperature variations. *Frontiers in Earth Science*, *11*. https://doi.org/10.3389/feart.2023.1307569

Chow, A. T., Tsai, K.-P., Fegel, T. S., Pierson, D. N., & Rhoades, C. C. (2019). Lasting effects of wildfire on disinfection by-product formation in forest catchments. *Journal of Environmental Quality*, *48*(6), 1826–1834. https://doi.org/10.2134/jeq2019.04.0172

Coble, P. G. (1996). Characterization of marine and terrestrial DOM in seawater using excitation-emission matrix spectroscopy. *Marine Chemistry*, *51*(4), 325–346. https://doi.org/10.1016/0304-4203(95)00062-3

Cole, J. J., Prairie, Y. T., Caraco, N. F., McDowell, W. H., Tranvik, L. J., Striegl, R. G., et al. (2007). Plumbing the global carbon cycle: Integrating inland waters into the terrestrial carbon Budget. *Ecosystems*, *10*(1), 172–185. https://doi.org/10.1007/s10021-006-9013-8

Condon, K. E. (2013). *Quantifying catchment-scale Particulate Organic Matter (POM) loss following fire, relative to background POM fluxes (M.S.)*. University of Arizona. Retrieved from http://hdl.handle.net/10150/301557

Cotrufo, M. F., Boot, C. M., Kampf, S., Nelson, P. A., Brogan, D. J., Covino, T., et al. (2016). Redistribution of pyrogenic carbon from hillslopes to stream corridors following a large montane wildfire. *Global Biogeochemical Cycles*, *30*(9), 1348–1355. https://doi.org/10.1002/2016GB005467

Crandall, T., Jones, E., Greenhalgh, M., Frei, R. J., Griffin, N., Severe, E., et al. (2021). Megafire affects stream sediment flux and dissolved organic matter reactivity, but land use dominates nutrient dynamics in semiarid watersheds. *PLoS One*, *16*(9), e0257733. https://doi.org/10.1371/journal.pone.0257733

Creed, I. F., McKnight, D. M., Pellerin, B. A., Green, M. B., Bergamaschi, B. A., Aiken, G. R., et al. (2015). The river as a chemostat: Fresh perspectives on dissolved organic matter flowing down the River continuum. *Canadian Journal of Fisheries and Aquatic Sciences*, *72*(8), 1272–1285. https://doi.org/10.1139/cjfas-2014-0400

Daly, C. (2024). Meteorological data from Primet (NOAHIV) at the Andrews forest [Dataset]. https://andrewsforest.oregonstate.edu/sites/default/files/lter/data/weather/portal/PRIMET/data/primet_or10_15min_merged.html

D'Andrilli, J., Junker, J. R., Smith, H. J., Scholl, E. A., & Foreman, C. M. (2019). DOM composition alters ecosystem function during microbial processing of isolated sources. *Biogeochemistry*, *142*(2), 281–298. https://doi.org/10.1007/s10533-018-00534-5

DeFrancesco, C., & Guéguen, C. (2021). Long-term trends in dissolved organic matter composition and its relation to sea ice in the Canada basin, Arctic Ocean (2007–2017). *Journal of Geophysical Research: Oceans*, *126*(2), e2020JC016578. https://doi.org/10.1029/2020JC016578

Derrien, M., Lee, M.-H., Choi, K., Lee, K.-S., & Hur, J. (2020). Tracking the evolution of particulate organic matter sources during summer storm events via end-member mixing analysis based on spectroscopic proxies. *Chemosphere*, *252*, 126445. https://doi.org/10.1016/j.chemosphere.2020.126445

Dewitz, J. (2021). National Land Cover Database (NLCD) 2019 products [Dataset]. *Science*. https://doi.org/10.5066/P9KZCM54

Drake, T. W., Raymond, P. A., & Spencer, R. G. M. (2018). Terrestrial carbon inputs to inland waters: A current synthesis of estimates and uncertainty. *Limnology and Oceanography Letters*, *3*(3), 132–142. https://doi.org/10.1002/lol2.10055

Dumelle, M., Peterson, E. E., Hoef, J. M. V., Pearse, A., & Isaak, D. J. (2024). SSN2: The next generation of spatial stream network modeling in R. *Journal of Open Source Software*, *9*(99), 6389. https://doi.org/10.21105/joss.06389

Ebel, B. A., & Moody, J. A. (2017). Synthesis of soil-hydraulic properties and infiltration timescales in wildfire-affected soils. *Hydrological Processes*, *31*(2), 324–340. https://doi.org/10.1002/hyp.10998

Egan, J. K., McKnight, D. M., Bowman, M. M., SanClements, M. D., Gallo, A. C., Hatten, J. A., & Matosziuk, L. M. (2023). Identifying photochemical alterations of dissolved pyrogenic organic matter using fluorescence spectroscopy. *Aquatic Sciences*, *85*(2), 38. https://doi.org/10.1007/s00027-022-00919-7

Fahey, T. J., Siccama, T. G., Driscoll, C. T., Likens, G. E., Campbell, J., Johnson, C. E., et al. (2005). The biogeochemistry of carbon at Hubbard Brook. *Biogeochemistry*, *75*(1), 109–176. https://doi.org/10.1007/s10533-004-6321-y

Fellman, J. B., D'Amore, D. V., & Hood, E. (2008). An evaluation of freezing as a preservation technique for analyzing dissolved organic C, N and P in surface water samples. *Science of the Total Environment*, *392*(2), 305–312. https://doi.org/10.1016/j.scitotenv.2007.11.027

Fernández-Pascual, E., Droz, B., O'Dwyer, J., O'Driscoll, C., Goslan, E. H., Harrison, S., & Weatherill, J. (2023). Fluorescent dissolved organic matter components as surrogates for disinfection byproduct formation in drinking water: A critical review. *ACS ES&T Water*, *3*(8), 1997–2008. https://doi.org/10.1021/acsestwater.2c00583

Fischer, S. J., Fegel, T. S., Wilkerson, P. J., Rivera, L., Rhoades, C. C., & Rosario-Ortiz, F. L. (2023). Fluorescence and absorbance indices for dissolved organic matter from wildfire Ash and burned watersheds. *ACS ES&T Water*, *3*(8), 2199–2209. https://doi.org/10.1021/acsestwater.3c00017

Forbes, M. S., Raison, R. J., & Skjemstad, J. O. (2006). Formation, transformation and transport of black carbon (charcoal) in terrestrial and aquatic ecosystems. *Science of the Total Environment*, *370*(1), 190–206. https://doi.org/10.1016/j.scitotenv.2006.06.007

Fox, B. G., Thorn, R. M. S., Anesio, A. M., Cox, T., Attridge, J. W., & Reynolds, D. M. (2019). Microbial processing and production of aquatic fluorescent organic matter in a model freshwater system. *Water*, *11*(1), 10. https://doi.org/10.3390/w11010010

Fuß, T., Behounek, B., Ulseth, A. J., & Singer, G. A. (2017). Land use controls stream ecosystem metabolism by shifting dissolved organic matter and nutrient regimes. *Freshwater Biology*, *62*(3), 582–599. https://doi.org/10.1111/fwb.12887

Giambastiani, B. M. S., Greggio, N., Nobili, G., Dinelli, E., & Antonellini, M. (2018). Forest fire effects on groundwater in a coastal aquifer (Ravenna, Italy). *Hydrological Processes*, *32*(15), 2377–2389. https://doi.org/10.1002/hyp.13165

Graeber, D., Gelbrecht, J., Pusch, M. T., Anlanger, C., & von Schiller, D. (2012). Agriculture has changed the amount and composition of dissolved organic matter in Central European headwater streams. *Science of the Total Environment*, *438*, 435–446. https://doi.org/10.1016/j.scitotenv.2012.08.087

Hallema, D. W., Sun, G., Bladon, K. D., Norman, S. P., Caldwell, P. V., Liu, Y., & McNulty, S. G. (2017). Regional patterns of postwildfire streamflow response in the Western United States: The importance of scale-specific connectivity. *Hydrological Processes*, *31*(14), 2582–2598. https://doi.org/10.1002/hyp.11208

Harjung, A., Schweichhart, J., Rasch, G., & Griebler, C. (2023). Large-scale study on groundwater dissolved organic matter reveals a strong heterogeneity and a complex microbial footprint. *Science of the Total Environment*, *854*, 158542. https://doi.org/10.1016/j.scitotenv.2022.158542

Hatten, J. A., & Zabowski, D. (2010). Fire severity effects on soil organic matter from a ponderosa pine forest: A laboratory study. *International Journal of Wildland Fire*, *19*(5), 613–623. https://doi.org/10.1071/WF08048

Hernes, P. J., Bergamaschi, B. A., Eckard, R. S., & Spencer, R. G. M. (2009). Fluorescence-based proxies for lignin in freshwater dissolved organic matter. *Journal of Geophysical Research*, *114*(G4). https://doi.org/10.1029/2009JG000938

Hickenbottom, K., Pagilla, K., & Hanigan, D. (2023). Wildfire impact on disinfection byproduct precursor loading in mountain streams and rivers. *Water Research*, *244*, 120474. https://doi.org/10.1016/j.watres.2023.120474

Hohner, A. K., Cawley, K., Oropeza, J., Summers, R. S., & Rosario-Ortiz, F. L. (2016). Drinking water treatment response following a Colorado wildfire. *Water Research*, *105*, 187–198. https://doi.org/10.1016/j.watres.2016.08.034

Hood, E., Gooseff, M. N., & Johnson, S. L. (2006). Changes in the character of stream water dissolved organic carbon during flushing in three small watersheds, Oregon. *Journal of Geophysical Research*, *111*(G1). https://doi.org/10.1029/2005JG000082

Hosen, J. D., McDonough, O. T., Febria, C. M., & Palmer, M. A. (2014). Dissolved organic matter quality and bioavailability changes across an Urbanization gradient in headwater streams. *Environmental Science & Technology*, *48*(14), 7817–7824. https://doi.org/10.1021/es501422z

Hrelja, I., Šestak, I., Delač, D., Pereira, P., & Bogunović, I. (2022). Soil chemical properties and trace elements after wildfire in mediterranean Croatia: Effect of severity, vegetation type and time-since-fire. *Agronomy*, *12*(7), 1515. https://doi.org/10.3390/agronomy12071515

Huang, M., Zhou, M., Li, Z., Ding, X., Wen, J., Jin, C., et al. (2022). How do drying-wetting cycles influence availability of heavy metals in sediment? A perspective from DOM molecular composition. *Water Research*, *220*, 118671. https://doi.org/10.1016/j.watres.2022.118671

Inamdar, S., & Mitchell, M. J. (2006). Hydrologic and topographic controls on storm-event exports of Dissolved Organic Carbon (DOC) and nitrate across catchment scales. *Water Resources Research*, *42*(3). https://doi.org/10.1029/2005WR004212

Inamdar, S., Singh, S., Dutta, S., Levia, D., Mitchell, M., Scott, D., et al. (2011). Fluorescence characteristics and sources of dissolved organic matter for stream water during storm events in a forested mid-Atlantic watershed. *Journal of Geophysical Research*, *116*(G3), G03043. https://doi.org/10.1029/2011JG001735

Ishii, S. K. L., & Boyer, T. H. (2012). Behavior of reoccurring PARAFAC components in fluorescent dissolved organic matter in natural and engineered systems: A critical review. *Environmental Science & Technology*, *46*(4), 2006–2017. https://doi.org/10.1021/es2043504

Jefferson, A., Grant, G., & Rose, T. (2006). Influence of volcanic history on groundwater patterns on the west slope of the Oregon High Cascades. *Water Resources Research*, *42*(12), W12411. https://doi.org/10.1029/2005WR004812

Jung, H. Y., Hogue, T. S., Rademacher, L. K., & Meixner, T. (2009). Impact of wildfire on source water contributions in Devil Creek, CA: Evidence from end-member mixing analysis. *Hydrological Processes*, *23*(2), 183–200. https://doi.org/10.1002/hyp.7132

Kagan, J., Gaines, E., Bernert, J., & Henderson, E. (2019). Oregon statewide habitat map–2018 [Dataset]. *GEOHub Data*. Retrieved from https://geohub.oregon.gov/documents/894a627ba88b45b89d91ed37bc347365/about

Kalbitz, K., Solinger, S., Park, J.-H., Michalzik, B., & Matzner, E. (2000). Controls on the dynamics of dissolved organic matter in soils: A review. *Soil Science*, *165*(4), 277–304. https://doi.org/10.1097/00010694-200004000-00001

Kalogirou, S., & Georganos, S. (2024). SpatialML: Spatial Machine Learning (version 0.1.7). Retrieved from https://cran.r-project.org/web/packages/SpatialML/index.html

Kang, H., Cole, R. P., Miralha, L., Compton, J. E., & Bladon, K. D. (2024). Hydrologic responses to wildfires in western Oregon, USA. *Journal of Hydrology*, *639*, 131612. https://doi.org/10.1016/j.jhydrol.2024.131612

Kim, J., Song, B.-C., & Kim, T.-H. (2022). Origin of dissolved organic carbon under phosphorus-limited coastal-bay conditions revealed by fluorescent dissolved organic matter. *Frontiers in Marine Science*, *9*. https://doi.org/10.3389/fmars.2022.971550

Kinoshita, A. M., & Hogue, T. S. (2015). Increased dry season water yield in burned watersheds in Southern California. *Environmental Research Letters*, *10*(1), 014003. https://doi.org/10.1088/1748-9326/10/1/014003

Knicker, H. (2007). How does fire affect the nature and stability of soil organic nitrogen and carbon? A review. *Biogeochemistry*, *85*(1), 91–118. https://doi.org/10.1007/s10533-007-9104-4

Kopp, B. J., Lange, J., & Menzel, L. (2017). Effects of wildfire on runoff generating processes in northern Mongolia. *Regional Environmental Change*, *17*(7), 1951–1963. https://doi.org/10.1007/s10113-016-0962-y

Kothawala, D. N., Roehm, C., Blodau, C., & Moore, T. R. (2012). Selective adsorption of dissolved organic matter to mineral soils. *Geoderma*, *189–190*, 334–342. https://doi.org/10.1016/j.geoderma.2012.07.001

Kothawala, D. N., Stedmon, C. A., Müller, R. A., Weyhenmeyer, G. A., Köhler, S. J., & Tranvik, L. J. (2014). Controls of dissolved organic matter quality: Evidence from a large-scale boreal lake survey. *Global Change Biology*, *20*(4), 1101–1114. https://doi.org/10.1111/gcb.12488

Lambert, T., Bouillon, S., Darchambeau, F., Massicotte, P., & Borges, A. V. (2016). Shift in the chemical composition of dissolved organic matter in the Congo River network. *Biogeosciences*, *13*(18), 5405–5420. https://doi.org/10.5194/bg-13-5405-2016

Lambert, T., Bouillon, S., Darchambeau, F., Morana, C., Roland, F. A. E., Descy, J.-P., & Borges, A. V. (2017). Effects of human land use on the terrestrial and aquatic sources of fluvial organic matter in a temperate river basin (The Meuse River, Belgium). *Biogeochemistry*, *136*(2), 191–211. https://doi.org/10.1007/s10533-017-0387-9

Larouche, J. R., Abbott, B. W., Bowden, W. B., & Jones, J. B. (2015). The role of watershed characteristics, permafrost thaw, and wildfire on dissolved organic carbon biodegradability and water chemistry in Arctic headwater streams. *Biogeosciences*, *12*(14), 4221–4233. https://doi.org/10.5194/bg-12-4221-2015

Lee, B. S., & Lajtha, K. (2016). Hydrologic and forest management controls on dissolved organic matter characteristics in headwater streams of old-growth forests in the Oregon Cascades. *Forest Ecology and Management*, *380*, 11–22. https://doi.org/10.1016/j.foreco.2016.08.029

Lentile, L. B., Morgan, P., Hudak, A. T., Bobbitt, M. J., Lewis, S. A., Smith, A. M. S., & Robichaud, P. R. (2007). Post-fire burn severity and vegetation response following eight large wildfires across the western United States. *Fire Ecology*, *3*(1), 91–108. https://doi.org/10.4996/fireecology.0301091

Mahat, V., Silins, U., & Anderson, A. (2016). Effects of wildfire on the catchment hydrology in southwest Alberta. *Catena*, *147*, 51–60. https://doi.org/10.1016/j.catena.2016.06.040

Maie, N., Scully, N. M., Pisani, O., & Jaffé, R. (2007). Composition of a protein-like fluorophore of dissolved organic matter in coastal wetland and estuarine ecosystems. *Water Research*, *41*(3), 563–570. https://doi.org/10.1016/j.watres.2006.11.006

Majidzadeh, H., Uzun, H., Ruecker, A., Miller, D., Vernon, J., Zhang, H., et al. (2017). Extreme flooding mobilized dissolved organic matter from coastal forested wetlands. *Biogeochemistry*, *136*(3), 293–309. https://doi.org/10.1007/s10533-017-0394-x

Mann, P. J., Davydova, A., Zimov, N., Spencer, R. G. M., Davydov, S., Bulygina, E., et al. (2012). Controls on the composition and lability of dissolved organic matter in Siberia's Kolyma River basin. *Journal of Geophysical Research*, *117*(G1). https://doi.org/10.1029/2011JG001798

Marlon, J. R., Bartlein, P. J., Gavin, D. G., Long, C. J., Anderson, R. S., Briles, C. E., et al. (2012). Long-term perspective on wildfires in the western USA. *Proceedings of the National Academy of Sciences*, *109*(9), E535–E543. https://doi.org/10.1073/pnas.1112839109

McGuire, K. J., Torgersen, C. E., Likens, G. E., Buso, D. C., Lowe, W. H., & Bailey, S. W. (2014). Network analysis reveals multiscale controls on stream water chemistry. *Proceedings of the National Academy of Sciences*, *111*(19), 7030–7035. https://doi.org/10.1073/pnas.1404820111

McKnight, D. M., Boyer, E. W., Westerhoff, P. K., Doran, P. T., Kulbe, T., & Andersen, D. T. (2001). Spectrofluorometric characterization of dissolved organic matter for indication of precursor organic material and aromaticity. *Limnology & Oceanography*, *46*(1), 38–48. https://doi.org/10.4319/lo.2001.46.1.0038

Miesel, J. R., Hockaday, W. C., Kolka, R. K., & Townsend, P. A. (2015). Soil organic matter composition and quality across fire severity gradients in coniferous and deciduous forests of the southern boreal region. *Journal of Geophysical Research: Biogeosciences*, *120*(6), 1124–1141. https://doi.org/10.1002/2015JG002959

Mikkelson, K. M., Dickenson, E. R. V., Maxwell, R. M., McCray, J. E., & Sharp, J. O. (2013). Water-quality impacts from climate-induced forest die-off. *Nature Climate Change*, *3*(3), 218–222. https://doi.org/10.1038/nclimate1724

Mineau, M. M., Wollheim, W. M., Buffam, I., Findlay, S. E. G., Hall, R. O., Jr., Hotchkiss, E. R., et al. (2016). Dissolved organic carbon uptake in streams: A review and assessment of reach-scale measurements. *Journal of Geophysical Research: Biogeosciences*, *121*(8), 2019–2029. https://doi.org/10.1002/2015JG003204

Moody, J. A., & Martin, D. A. (2001). Initial hydrologic and geomorphic response following a wildfire in the Colorado Front Range. *Earth Surface Processes and Landforms*, *26*(10), 1049–1070. https://doi.org/10.1002/esp.253

MTBS Project. (2021). MTBS data access: Fire level geospatial data [Dataset]. *USDA Forest Service/U.S. Geological Survey*. Retrieved from http://mtbs.gov/direct-download

Mueller, K. K., Lofts, S., Fortin, C., & Campbell, P. G. C. (2012). Trace metal speciation predictions in natural aquatic systems: Incorporation of Dissolved Organic Matter (DOM) spectroscopic quality. *Environmental Chemistry*, *9*(4), 356–368. https://doi.org/10.1071/EN11156

Murphy, K. R., Stedmon, C. A., Graeber, D., & Bro, R. (2013). Fluorescence spectroscopy and multi-way techniques. PARAFAC. *Analytical Methods*, *5*(23), 6557–6566. https://doi.org/10.1039/C3AY41160E

Murphy, K. R., Stedmon, C. A., Wenig, P., & Bro, R. (2014). OpenFluor-an online spectral library of auto-fluorescence by organic compounds in the environment. *Analytical Methods*, *6*(3), 658–661. https://doi.org/10.1039/C3AY41935E

Oksanen, J., Simpson, G. L., Blanchet, F. G., Kindt, R., Legendre, P., Minchin, P. R., et al. (2024). Vegan: Community ecology package (version 2.6-6.1). Retrieved from https://cran.r-project.org/web/packages/vegan/index.html

Onda, Y., Dietrich, W. E., & Booker, F. (2008). Evolution of overland flow after a severe forest fire, Point Reyes, California. *Catena*, *72*(1), 13–20. https://doi.org/10.1016/j.catena.2007.02.003

Orlova, J., Amiri, F., Bourgeois, A. K., Buttle, J. M., Cherlet, E., Cuss, C. W., et al. (2024). Composition of stream dissolved organic matter across Canadian forested Ecozones Varies in three dimensions linked to landscape and climate. *Water Resources Research*, *60*(5), e2023WR035196. https://doi.org/10.1029/2023WR035196

Panettieri, M., Guigue, J., Chemidlin Prevost-Bouré, N., Thévenot, M., Lévêque, J., Le Guillou, C., et al. (2020). Grassland-cropland rotation cycles in crop-livestock farming systems regulate priming effect potential in soils through modulation of microbial communities, composition of soil organic matter and abiotic soil properties. *Agriculture, Ecosystems & Environment*, *299*, 106973. https://doi.org/10.1016/j.agee.2020.106973

Parham, L. M., Prokushkin, A. S., Pokrovsky, O. S., Titov, S. V., Grekova, E., Shirokova, L. S., & McDowell, W. H. (2013). Permafrost and fire as regulators of stream chemistry in basins of the Central Siberian Plateau. *Biogeochemistry*, *116*(1), 55–68. https://doi.org/10.1007/s10533-013-9922-5

Peterson, E., & Ver Hoef, J. M. (2014). Stars: An ArcGIS toolset used to calculate the spatial information needed to fit spatial statistical models to stream network data. *Journal of Statistical Software*, *56*(2), 1–17. https://doi.org/10.18637/jss.v056.i02

Preston, C. M., & Schmidt, M. W. I. (2006). Black (pyrogenic) carbon: A synthesis of current knowledge and uncertainties with special consideration of boreal regions. *Biogeosciences*, *3*(4), 397–420. https://doi.org/10.5194/bg-3-397-2006

PRISM Climate Group. (2024). 30-Year normals [Dataset]. *Oregon State University*. Retrieved from http://prism.oregonstate.edu

Pucher, M., Flödl, P., Graeber, D., Felsenstein, K., Hein, T., & Weigelhofer, G. (2021). Complex interactions of in-stream dissolved organic matter and nutrient spiralling unravelled by Bayesian regression analysis. *Biogeosciences*, *18*(10), 3103–3122. https://doi.org/10.5194/bg-18-3103-2021

Pucher, M., Wünsch, U., Weigelhofer, G., Murphy, K., Hein, T., & Graeber, D. (2019). staRdom: Versatile software for analyzing spectroscopic data of dissolved organic matter in R. *Water*, *11*, 2366. https://doi.org/10.3390/w11112366

Queimaliños, C., Reissig, M., Pérez, G. L., Soto Cárdenas, C., Gerea, M., Garcia, P. E., et al. (2019). Linking landscape heterogeneity with lake dissolved organic matter properties assessed through absorbance and fluorescence spectroscopy: Spatial and seasonal patterns in temperate lakes of Southern Andes (Patagonia, Argentina). *Science of the Total Environment*, *686*, 223–235. https://doi.org/10.1016/j.scitotenv.2019.05.396

Raoelison, O. D., Valenca, R., Lee, A., Karim, S., Webster, J. P., Poulin, B. A., & Mohanty, S. K. (2023). Wildfire impacts on surface water quality parameters: Cause of data variability and reporting needs. *Environmental Pollution*, *317*, 120713. https://doi.org/10.1016/j.envpol.2022.120713

Raymond, P. A., McClelland, J. W., Holmes, R. M., Zhulidov, A. V., Mull, K., Peterson, B. J., et al. (2007). Flux and age of dissolved organic carbon exported to the Arctic Ocean: A carbon isotopic study of the five largest arctic rivers. *Global Biogeochemical Cycles*, *21*(4). https://doi.org/10.1029/2007GB002934

Raymond, P. A., & Saiers, J. E. (2010). Event controlled DOC export from forested watersheds. *Biogeochemistry*, *100*(1), 197–209. https://doi.org/10.1007/s10533-010-9416-7

R Core Team. (2024). *R: A language and environment for statistical computing*. R Foundation for Statistical Computing. Retrieved from https://www.R-project.org/

Reitsema, R. E., Meire, P., & Schoelynck, J. (2018). The future of freshwater macrophytes in a changing world: Dissolved organic carbon quantity and quality and its interactions with macrophytes. *Frontiers in Plant Science*, *9*. https://doi.org/10.3389/fpls.2018.00629

Retelletti Brogi, S., Balestra, C., Casotti, R., Cossarini, G., Galletti, Y., Gonnelli, M., et al. (2020). Time resolved data unveils the complex DOM dynamics in a Mediterranean river. *Science of the Total Environment*, *733*, 139212. https://doi.org/10.1016/j.scitotenv.2020.139212

Retelletti Brogi, S., Jung, J. Y., Ha, S.-Y., & Hur, J. (2019). Seasonal differences in dissolved organic matter properties and sources in an Arctic fjord: Implications for future conditions. *Science of the Total Environment*, *694*, 133740. https://doi.org/10.1016/j.scitotenv.2019.133740

Revchuk, A. D., & Suffet, I. H. (2014). Effect of wildfires on physicochemical changes of watershed dissolved organic matter. *Water Environment Research*, *86*(4), 372–381. https://doi.org/10.2175/106143013X13736496909671

Rey, D. M., Briggs, M. A., Walvoord, M. A., & Ebel, B. A. (2023). Wildfire-induced shifts in groundwater discharge to streams identified with paired air and stream water temperature analyses. *Journal of Hydrology*, *619*, 129272. https://doi.org/10.1016/j.jhydrol.2023.129272

Rhea, A. E., Covino, T. P., & Rhoades, C. C. (2021). Reduced N-limitation and increased in-stream productivity of autotrophic biofilms 5 and 15 Years after severe wildfire. *Journal of Geophysical Research: Biogeosciences*, *126*(9), e2020JG006095. https://doi.org/10.1029/2020JG006095

Robinson, C. T., Uehlinger, U., & Minshall, G. W. (2005). Functional characteristics of wilderness streams twenty years following wildfire. *Western North American Naturalist*, *65*(1), 1–10.

Rodríguez, J., González-Pérez, J. A., Turmero, A., Hernández, M., Ball, A. S., González-Vila, F. J., & Enriqueta Arias, M. (2017). Wildfire effects on the microbial activity and diversity in a Mediterranean forest soil. *Catena*, *158*, 82–88. https://doi.org/10.1016/j.catena.2017.06.018

Rodríguez-Cardona, B. M., Coble, A. A., Wymore, A. S., Kolosov, R., Podgorski, D. C., Zito, P., et al. (2020). Wildfires lead to decreased carbon and increased nitrogen concentrations in upland Arctic streams. *Scientific Reports*, *10*(1), 8722. https://doi.org/10.1038/s41598-020-65520-0

Roebuck, J. A., Jr., Bladon, K. D., Donahue, D., Graham, E. B., Grieger, S., Morgenstern, K., et al. (2022). Spatiotemporal controls on the delivery of dissolved organic matter to streams following a wildfire. *Geophysical Research Letters*, *49*(16), e2022GL099535. https://doi.org/10.1029/2022GL099535

Roebuck, J. A., Jr., Grieger, S., Barnes, M. E., Gillespie, X., Bladon, K. D., Bailey, J. D., et al. (2024). Molecular shifts in dissolved organic matter along a burn severity continuum for common land cover types in the Pacific Northwest, USA. *SSRN Scholarly Paper*. Retrieved from https://papers.ssrn.com/abstract=4915022

Roth, V.-N., Lange, M., Simon, C., Hertkorn, N., Bucher, S., Goodall, T., et al. (2019). Persistence of dissolved organic matter explained by molecular changes during its passage through soil. *Nature Geoscience*, *12*(9), 755–761. https://doi.org/10.1038/s41561-019-0417-4

Santín, C., Doerr, S. H., Otero, X. L., & Chafer, C. J. (2015). Quantity, composition and water contamination potential of ash produced under different wildfire severities. *Environmental Research*, *142*, 297–308. https://doi.org/10.1016/j.envres.2015.06.041

Santos, F., Wymore, A. S., Jackson, B. K., Sullivan, S. M. P., McDowell, W. H., & Berhe, A. A. (2019). Fire severity, time since fire, and site-level characteristics influence stream water chemistry at baseflow conditions in catchments of the Sierra Nevada, California, USA. *Fire Ecology*, *15*(1), 3. https://doi.org/10.1186/s42408-018-0022-8

Schwarz, G. E., Jackson, S. E., & Wieczorek, M. E. (2018). Select attributes for NHDPlus version 2.1 reach catchments and modified network routed upstream watersheds for the conterminous United States (ver. 4.0, August 2023) [Dataset]. *U.S. Geological Survey*. https://doi.org/10.5066/F7765D7V

Shen, Y., Chapelle, F. H., Strom, E. W., & Benner, R. (2015). Origins and bioavailability of dissolved organic matter in groundwater. *Biogeochemistry*, *122*(1), 61–78. https://doi.org/10.1007/s10533-014-0029-4

Shutova, Y., Baker, A., Bridgeman, J., & Henderson, R. K. (2014). Spectroscopic characterisation of dissolved organic matter changes in drinking water treatment: From PARAFAC analysis to online monitoring wavelengths. *Water Research*, *54*, 159–169. https://doi.org/10.1016/j.watres.2014.01.053

Singh, A. K., Kushwaha, M., Rai, A., & Singh, N. (2017). Changes in soil microbial response across year following a wildfire in tropical dry forest. *Forest Ecology and Management*, *391*, 458–468. https://doi.org/10.1016/j.foreco.2017.02.042

Singh, S., Inamdar, S., Mitchell, M., & McHale, P. (2014). Seasonal pattern of Dissolved Organic Matter (DOM) in watershed sources: Influence of hydrologic flow paths and autumn leaf fall. *Biogeochemistry*, *118*(1–3), 321–337. https://doi.org/10.1007/s10533-013-9934-1

Smakhtin, V. U. (2001). Low flow hydrology: A review. *Journal of Hydrology*, *240*(3), 147–186. https://doi.org/10.1016/S0022-1694(00)00340-1

Stedmon, C. A., & Markager, S. (2005a). Resolving the variability in dissolved organic matter fluorescence in a temperate estuary and its catchment using PARAFAC analysis. *Limnology & Oceanography*, *50*(2), 686–697. https://doi.org/10.4319/lo.2005.50.2.0686

Stedmon, C. A., & Markager, S. (2005b). Tracing the production and degradation of autochthonous fractions of dissolved organic matter by fluorescence analysis. *Limnology & Oceanography*, *50*(5), 1415–1426. https://doi.org/10.4319/lo.2005.50.5.1415

Stedmon, C. A., Markager, S., & Bro, R. (2003). Tracing dissolved organic matter in aquatic environments using a new approach to fluorescence spectroscopy. *Marine Chemistry*, *82*(3), 239–254. https://doi.org/10.1016/S0304-4203(03)00072-0

Stedmon, C. A., Markager, S., Tranvik, L., Kronberg, L., Slätis, T., & Martinsen, W. (2007). Photochemical production of ammonium and transformation of dissolved organic matter in the Baltic Sea. *Marine Chemistry*, *104*(3), 227–240. https://doi.org/10.1016/j.marchem.2006.11.005

Stoof, C. R., Slingerland, E. C., Mol, W., van den Berg, J., Vermeulen, P. J., Ferreira, A. J. D., et al. (2014). Preferential flow as a potential mechanism for fire-induced increase in streamflow. *Water Resources Research*, *50*(2), 1840–1845. https://doi.org/10.1002/2013WR014397

Tague, C., & Grant, G. E. (2004). A geological framework for interpreting the low-flow regimes of Cascade streams, Willamette River Basin, Oregon. *Water Resources Research*, *40*(4). https://doi.org/10.1029/2003WR002629

Tetzlaff, D., Seibert, J., McGuire, K. J., Laudon, H., Burns, D. A., Dunn, S. M., & Soulsby, C. (2009). How does landscape structure influence catchment transit time across different geomorphic provinces? *Hydrological Processes*, *23*(6), 945–953. https://doi.org/10.1002/hyp.7240

Thuile Bistarelli, L., Poyntner, C., Santín, C., Doerr, S. H., Talluto, M. V., Singer, G., & Sigmund, G. (2021). Wildfire-derived pyrogenic carbon modulates riverine organic matter and biofilm enzyme activities in an in situ flume experiment. *ACS ES & T Water*, *1*(7), 1648–1656. https://doi.org/10.1021/acsestwater.1c00185

Thygesen, L. G., Rinnan, Å., Barsberg, S., & Møller, J. K. S. (2004). Stabilizing the PARAFAC decomposition of fluorescence spectra by insertion of zeros outside the data area. *Chemometrics and Intelligent Laboratory Systems*, *71*(2), 97–106. https://doi.org/10.1016/j.chemolab.2003.12.012

Trabucco, A., & Zomer, R. (2019). Global aridity index and potential Evapotranspiration (ET0) [Dataset]. *Climate Database v2*. https://doi.org/10.6084/m9.figshare.7504448.v3

Tshering, K., Miotlinski, K., Blake, D., Boyce, M. C., Bath, A., Carvalho, A., & Horwitz, P. (2023). Effect of fire on characteristics of dissolved organic matter in forested catchments in the Mediterranean biome: A review. *Water Research*, *230*, 119490. https://doi.org/10.1016/j.watres.2022.119490

Tuckett, Q. M., & Koetsier, P. (2016). Mid- and long-term effects of wildfire and debris flows on stream ecosystem metabolism. *Freshwater Science*, *35*(2), 445–456. https://doi.org/10.1086/686151

Tupas, L. M., Popp, B. N., & Karl, D. M. (1994). Dissolved organic carbon in oligotrophic waters: Experiments on sample preservation, storage and analysis. *Marine Chemistry*, *45*(3), 207–216. https://doi.org/10.1016/0304-4203(94)90004-3

U.S. Geological Survey. (2003). Base-flow index grid for the conterminous United States [Dataset]. https://water.usgs.gov/GIS/metadata/usgswrd/XML/bfi48grd.xml

USDA NRCS. (2016). Oregon SSURGO STATSGO soils compilation [Dataset]. https://spatialdata.oregonexplorer.info/geoportal/details;id=668a7a8824e5456797bec858cc14ca74

Uselman, S. M., Qualls, R. G., & Lilienfein, J. (2012). Quality of soluble organic C, N, and P produced by different types and species of litter: Root litter versus leaf litter. *Soil Biology and Biochemistry*, *54*, 57–67. https://doi.org/10.1016/j.soilbio.2012.03.021

U.S. Geological Survey. (2000). Shuttle Radar Topography Mission (SRTM) 1 arc-second global [Dataset]. https://doi.org/10.5066/F7PR7TFT

U.S. Geological Survey. (2019). The StreamStats program. Retrieved from https://streamstats.usgs.gov/ss/

U.S. Geological Survey. (2020). National Hydrography Dataset (NHD)—USGS National map downloadable data collection [Dataset]. https://www.usgs.gov/national-hydrography/national-hydrography-dataset

Uzun, H., Dahlgren, R. A., Olivares, C., Erdem, C. U., Karanfil, T., & Chow, A. T. (2020). Two years of post-wildfire impacts on dissolved organic matter, nitrogen, and precursors of disinfection by-products in California stream waters. *Water Research*, *181*, 115891. https://doi.org/10.1016/j.watres.2020.115891

van Verseveld, W. J., McDonnell, J. J., & Lajtha, K. (2008). A mechanistic assessment of nutrient flushing at the catchment scale. *Journal of Hydrology*, *358*(3), 268–287. https://doi.org/10.1016/j.jhydrol.2008.06.009

Ver Hoef, J. M., Peterson, E., & Theobald, D. (2006). Spatial statistical models that use flow and stream distance. *Environmental and Ecological Statistics*, *13*(4), 449–464. https://doi.org/10.1007/s10651-006-0022-8

Ver Hoef, J. M., & Peterson, E. E. (2010). A moving average approach for spatial statistical models of stream networks. *Journal of the American Statistical Association*, *105*(489), 6–18. https://doi.org/10.1198/jasa.2009.ap08248

Wagner, S., Cawley, K. M., Rosario-Ortiz, F. L., & Jaffé, R. (2015). In-stream sources and links between particulate and dissolved black carbon following a wildfire. *Biogeochemistry*, *124*(1), 145–161. https://doi.org/10.1007/s10533-015-0088-1

Wagner, S., & Jaffé, R. (2015). Effect of photodegradation on molecular size distribution and quality of dissolved black carbon. *Organic Geochemistry*, *86*, 1–4. https://doi.org/10.1016/j.orggeochem.2015.05.005

Wagner, S., Jaffé, R., & Stubbins, A. (2018). Dissolved black carbon in aquatic ecosystems. *Limnology and Oceanography Letters*, *3*(3), 168–185. https://doi.org/10.1002/lol2.10076

Wampler, K. A. (2023). Fewsdom: Tools to process data from Horiba Aqualog (version 0.1.0). Retrieved from https://katiewampler.github.io/fewsdom/

Wampler, K. A., Bladon, K. D., & Myers-Pigg, A. N. (2024a). Data and scripts describing dissolved organic matter character across a stream network in Oregon following the 2020 Holiday Farm Wildfire [Dataset]. *ScholarsArchive@OSU*. Retrieved from https://ir.library.oregonstate.edu/concern/datasets/mc87q034m

Wampler, K. A., Bladon, K. D., & Myers-Pigg, A. N. (2024b). McKenzie_21_24 [Dataset]. https://openfluor.lablicate.com/:OpenFluor

Wampler, K. A., Bladon, K. D., & Myers-Pigg, A. N. (2024c). The influence of burn severity on dissolved organic carbon concentrations across a stream network differs based on seasonal wetness conditions. *Biogeosciences*, *21*(13), 3093–3120. https://doi.org/10.5194/bg-21-3093-2024

Wampler, K. A., Boise, N. R., Donahue, D., Erkert, L., Forbes, B., Fricke, S., et al. (2024). Organic matter concentration and composition in November 2021 and April 2022 from 12 streams impacted by the 2020 Holiday Farm [Dataset]. *ESS-DIVE*. https://doi.org/10.15485/2478546

Wasserman, T. N., & Mueller, S. E. (2023). Climate influences on future fire severity: A synthesis of climate-fire interactions and impacts on fire regimes, high-severity fire, and forests in the western United States. *Fire Ecology*, *19*(1), 43. https://doi.org/10.1186/s42408-023-00200-8

Wheeler, K. I., Levia, D. F., & Hudson, J. E. (2017). Tracking senescence-induced patterns in leaf litter leachate using Parallel Factor Analysis (PARAFAC) modeling and self-organizing maps. *Journal of Geophysical Research: Biogeosciences*, *122*(9), 2233–2250. https://doi.org/10.1002/2016JG003677

Williams, C. H. S., Silins, U., Spencer, S. A., Wagner, M. J., Stone, M., & Emelko, M. B. (2019). Net precipitation in burned and unburned subalpine forest stands after wildfire in the northern Rocky Mountains. *International Journal of Wildland Fire*, *28*(10), 750–760. https://doi.org/10.1071/WF18181

Wünsch, U. J., Murphy, K. R., & Stedmon, C. A. (2017). The One-sample PARAFAC approach reveals molecular size distributions of fluorescent components in dissolved organic matter. *Environmental Science & Technology*, *51*(20), 11900–11908. https://doi.org/10.1021/acs.est.7b03260

Yamashita, Y., Kloeppel, B. D., Knoepp, J., Zausen, G. L., & Jaffé, R. (2011). Effects of watershed history on dissolved organic matter characteristics in headwater streams. *Ecosystems*, *14*(7), 1110–1122. https://doi.org/10.1007/s10021-011-9469-z

Yang, L., Hur, J., & Zhuang, W. (2015). Occurrence and behaviors of fluorescence EEM-PARAFAC components in drinking water and wastewater treatment systems and their applications: A review. *Environmental Science and Pollution Research*, *22*(9), 6500–6510. https://doi.org/10.1007/s11356-015-4214-3

Yin, G., Guan, P., Wang, Y.-H., Zhang, P., Qu, B., Xu, S., et al. (2024). Temporal variations in fire impacts on characteristics and composition of soil-derived dissolved organic matter at Qipan mountain, China. *Environmental Science & Technology*, *58*(31), 13772–13782. https://doi.org/10.1021/acs.est.4c00446

Zhang, F., Li, X., Duan, L., Zhang, H., Gu, W., Yang, X., et al. (2021). Effect of different DOM components on arsenate complexation in natural water. *Environmental Pollution*, *270*, 116221. https://doi.org/10.1016/j.envpol.2020.116221

Zhang, Q., Wang, Y., Guan, P., Zhang, P., Mo, X., Yin, G., et al. (2023). Temperature thresholds of pyrogenic dissolved organic matter in heating experiments simulating forest fires. *Environmental Science & Technology*, *57*(45), 17291–17301. https://doi.org/10.1021/acs.est.3c05265

Zhou, L., Zhou, Y., Tang, X., Zhang, Y., Jang, K.-S., Székely, A. J., & Jeppesen, E. (2021). Resource aromaticity affects bacterial community successions in response to different sources of dissolved organic matter. *Water Research*, *190*, 116776. https://doi.org/10.1016/j.watres.2020.116776

Zhou, Y., Martin, P., & Müller, M. (2019). Composition and cycling of dissolved organic matter from tropical peatlands of coastal Sarawak, Borneo, revealed by fluorescence spectroscopy and parallel factor analysis. *Biogeosciences*, *16*(13), 2733–2749. https://doi.org/10.5194/bg-16-2733-2019

Zimmerman, D. L., & Ver Hoef, J. M. (2017). The Torgegram for fluvial Variography: Characterizing spatial dependence on stream networks. *Journal of Computational & Graphical Statistics*, *26*(2), 253–264. https://doi.org/10.1080/10618600.2016.1247006